University of Liverpool

MATH 554: Main Summer Dissertation

Modelling chemotactic motion of self-repelling group of cells

Author:
Nor Zubaidah Hassan

Supervisor:
Dr. Bakhti Vasiev

September 14, 2012

Contents

1 Introduction

Embryonic development has always been an area of extreme interest to biologist. Important cellular events occurring during embryonic development, such as cell differentiation, proliferation and migration of cells are amongst the areas which has been or being analysed by biologist. They look for appropriate tools to systematically analyse their experimental data. For instance, in cell differentiation, on the basis of the vast amount of experimental observations, it was concluded that the cells differentiate according to their location in the embryo and the positional information is provided by the so-called "morphogen gradient". This term refers to the substance which is present and non-uniformly distributed in the embryo and cells, composing the embryo and differentiates according to its dynamics and local concentration.

The word "gradient" is a mathematical term to denote a vector representing the rate of change over space in biology. It refers to the inhomogeneous distribution of the substance. This term was suggested by the biologist, Wolpert. As for the term "morphogen", it was named by the Mathematician, Turing, who studied formation of the chemical concentration profiles in mathematical models. Mathematical formulation of basic principles is indeed essential in driving morphogenesis.

In migration of cells, a comprehensive analysis of cell migration or movement patterns associated with the geometry of developing tissues have been made. However, little is known about mechanics of migration and rearrangement of cells in embryonic tissues. Probably the most common mechanism used by nature is **chemotaxis** when the migration of cell is driven by the gradient of a substance which is, in this case, called a chemotactic agent.

So what is chemotaxis?

Chemotaxis is a phenomenon whereby somatic cells, bacteria and other single-cell organisms direct their movements according to certain chemicals in their environment. History of chemotaxis research is indeed well known. Migration of cells was detected from the early days of the development of microscopy but erudite description of chemotaxis was first made by TW. Engelmann and W.F. Pfeffer in bacteria and H.S.Jennings in ciliates. The significance of chemotaxis in biology and clinical pathology was widely accepted in the 1930s [13].

Chemotaxis is important for bacteria to find food (for example glucose) by swimming towards the highest concentration of food molecules, or to flee from poisons (for example phenol). In multicellular organism, chemotaxis is critical to early development (for example the movement of sperm towards the egg during fertilization) and subsequent phases of development (for example the migration of neurons and lymphocytes) as well as in normal function. In addition, it has been recognized

that mechanisms that allow chemotaxis in animals can be subverted during cancer metastasis.

In bacterial chemotaxis, all of the genes and proteins involved have been identified and isolated, making this the most completely understood form of motile cell behaviour [10]. In the presence of a chemical gradient, bacteria will chemotax, or direct their overall motion based on the gradient. If the bacterium senses that it is moving in the correct direction, i.e. towards attractant or away from repellent, it will keep swimming in a straight line for a longer time before tumbling. If it is in the wrong direction, it will tumble sooner and try a new direction at random. Alternation between swimming and tumbling is influenced by the presence of chemoattractants and chemorepellents in the medium and forms the basis of the chemotactic response. In other words, bacteria like the *E.Coli* use temporal sensing to decide whether their situation is improving or not. In this way, it finds the location with the highest concentration of attractant (usually the source) quite well. Even under very high concentrations, it can still distinguish very small differences in concentration. Fleeing from a repellent works with the same efficiency. This purposeful random walk is a result of simply choosing between two methods of random movement; namely tumbling and straight swimming. In fact, chemotactic responses such as "forgetting direction" and "choosing movements" resemble the decision making abilities of higher life-forms with brains that process sensory data [9].

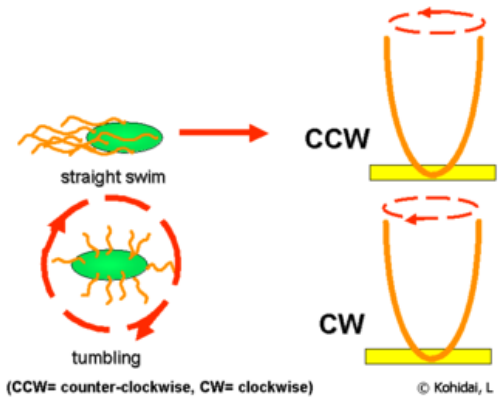

Figure 1: Correlation of swimming behaviour and flagellar rotation in *E.Coli*.

In eukaryotic chemotaxis, the mechanism employ is quite different from that in bacteria. However, sensing of chemical gradients is still a crucial step in the process. Due to their size, prokaryotes cannot detect effective concentration gradients, therefore these cells scan and evaluate their environment by a constant swimming

(consecutive steps of straight swims and tumbles). In contrast to prokaryotes, the size of eukaryotes cells allows the possibility of detecting gradients, which results in a dynamic and polarized distribution of receptors. Induction of these receptors by chemoattractants or chemorepellents results in migration towards or away from the chemotactic substance [13]. Study of eukaryotic cell migration and chemotaxis are processes which are fundamental to cell growth, survival and death.

Chemotaxis, in particular, is essential during embryonic development, immune cell function and cancer metastasis. It has high significance in the early phases of embryogenesis as development of germ layers is guided by gradients of signal molecules [2].

Chemotaxis does not exist independently. It is very much assisted by mathematical techniques. The use of mathematical techniques for classification and understanding of the ever-growing amount of experimental data and possible help in designing new experiments is now more profound than ever. Recently, mathematical modelling plays an uprising role in biological studies in general and in particular, in developmental biology. Mathematical modelling in developmental biology has an important role in helping us discover biophysical mechanics driving the development. It is a unique tool which allows a rigorous check of hypotheses concerning these mechanisms as they emerge from the experimental observations.

Several mathematical models of chemotaxis was developed depending (among which) on the type of

(a) migration (for examples the basic differences of bacterial swimming, movement of unicellular eukaryotes with cilia/flagellum and amoeboid migration),

(b) assay systems applied to evaluate chemotaxis (to see incubation times, development and stability of concentration gradients) and

(c) other environmental effects possessing direct or indirect influence on the migration (lighting, temperature, magnetic fields, etc.)

Other publications written in genetics, biochemistry, cell physiology, pathology and clinical sciences could also incorporate data about migration or especially the chemotaxis of cells. A curiosity of migration research is that among several works investigating taxes (for examples thermotaxis, geotaxis and phototaxis), chemotaxis research shows a significantly high ratio, which point to the underlined importance of chemotaxis research both in biology and medicine [13].

For chemotaxis, a mathematical description for it requires a model to describe the cells ability to sense a gradient of ambient chemoattractant and its interaction with a physical model of cell migration. It is also now appreciated that it is important

to model the feedback from the evolving cell shape and the intra and extra cell signalling pathways which lead to directed cell motion. The computational challenge therefore involves the solution of partial differential equations (PDEs) on evolving surfaces where the computed solution state is used to derive movement and changes in cell shape.

Further chemotaxis uses a *non-linear model*. Contrary to linear models, which have a limited range of possible solutions, non-linear models can be used to reproduce virtually any kind of known dynamics in concentration fields of morphogens. This is especially true if more than one morphogen is considered. The model is represented by a so called *reaction-diffusion equations* (It is used to derive the equation for the flux of cells whose motion is affected by variations in the ambient concentration of certain chemicals) [7].

An individual cell path can result in an average cell flux which is proportional to the macroscopic chemical gradient. We let $b(x)$ denote the density of cells centred at x and we will find $J(x)$, the net flux of cells per unit time in the direction of increasing x. The dependence of cell density $b(x,t)$ on position and time is described by the differential equation

$$\frac{\partial b}{\partial t} = -\nabla \cdot J,$$

where the vector flux J would be given by

$$J = -\mu \nabla b + \chi \nabla c.$$

The first term is the *diffusion* term, describing the non-chemotactic, random motion of cells, and the second term describes the *chemotactic response*.

The diffusion or 'motility coefficient', μ, is given by

$$\mu(c) \equiv \frac{\Delta^2}{\Delta t} = f(c)\Delta^2,$$

where $\Delta t \equiv \frac{1}{f(c)}$ is the average time interval between steps. Similarly, χ, the chemotactic coefficient, is given by

$$\chi(c) = (\alpha - 1) f'(c) \Delta^2,$$

so that

$$\chi(c) \quad = \quad (\alpha - 1)\mu'(c).$$

Chemotaxis has been used in the detailed study of the developing population of *Dictyostelium discoideum (Dd) amoebae*. This biological object cooperates and show striking social behaviour when they are deprived of food. The starving cells then communicate by means of chemical signal to synchronise their otherwise random and unorganised movement.

The molecular machinery for cell motility is currently best understood in Dd. This is because it is an organism which spends most of its life as a chemotactic amoeboid phagocyte but which also uses chemotaxis to form a multicellular organism during subsequent stages of development. In this process of transformation, there is both production of and a chemotactic response to cyclic adenosine $3'$ - monophosphate (cAMP); the result is aggregation [8].

Aggregation of Dd amoebae is an example of a phenomenon whereby the wave of excitation can change the properties of excitable media and cause the formation of spatial patterns. The monolayer of the starving amoebae is an excitable medium which conducts excitation waves of the intracellular mediator i.e. the cAMP. Since cAMP is a chemotactic attractant for the amoebae, the waves of cAMP cause motion of the amoebae. As a result of this motion amoebae are organized into streams which usually form branching radial multicellular structures. There are two major types of cAMP sources forming aggregates: a point source and a spiral wave. Figure 2 shows streams which were induced by a spiral wave of cAMP.

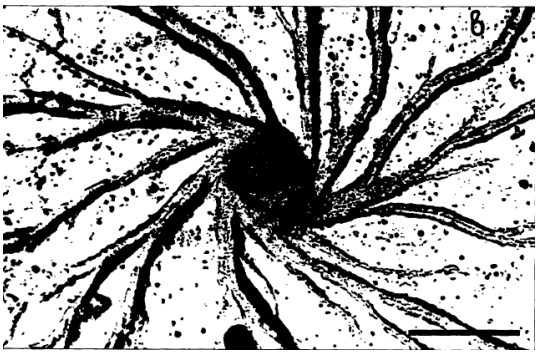

Figure 2: View of aggregative structure formed by a starving population of *Dictyostelium discoideum*.

The process of aggregation of Dd amoebae was numerically studied in a continuous model and thus the reaction-diffusion model was proposed for the simulation of the process. The model is based on *FitzHugh-Nagumo*-type equations for cAMP waves

and a continuity equation for amoebae motion. The process of aggregation induced was simulated by a periodic point source and by spiral wave. It was shown that aggregation pattern is formed as a result of front instabilities due to dependence of wave velocity on density of amoebae. This instability can also result in formation of wave breaks and generation of spiral waves.

For calculations, the following model was used:

$$\begin{aligned} \frac{\partial r}{\partial t} &= \frac{(g-r)}{\tau}\ , \\ \frac{\partial g}{\partial t} &= D_g \Delta g + c^{\alpha}(f(g) - K_r r), \\ \frac{\partial c}{\partial t} &= D_c \Delta c - \nabla(cV(r)\Delta g). \end{aligned} \tag{1}$$

The first two equations are a FitzHigh-Nagumo model which describes the propagation of cAMP waves. g represents the extracellular concentration of cAMP and r, the recovery process. Instead of ordinary cubic function, $f(g)$, in the 2$^{\text{nd}}$ equation, the piecewise linear function is used instead:

$$f(g) = \begin{cases} -S_g & \text{if} \quad g \leq 0, \\ K_g(g-a) & \text{if} \quad 0 < g < 1, \\ -S(g-1) & \text{if} \quad g \geq 0. \end{cases}$$

(S is infinite, $f(g)$ is only defined on the interval $0 < g < 1$). It was suggested that in normal conditions, the production and decay of cAMP are proportional to the cell density, $c^{\alpha}(\alpha = 1)$.

The 3$^{\text{rd}}$ equation in (1) describes the chemotactic motion of amoebae. c is the local concentration of amoebae, and $V(r)$ is their motility. In the model (as $r \geq 0$), V reaches its maximum at $r = 0$ and decreases to 0, with increasing r. Biologically, this means that cells move if they are not refractory (i.e. not able to respond to additional stimulation).

From an initially random distribution of amoebae, the formation of aggregation pattern will occur. They will form the pattern of branching streams. Therefore a necessary condition for stream formation is non-uniformity in the initial distribution of amoebae density. If a computation is done, but with an initially uniform distribution of amoebae instead, streams will not be formed. Amoebae collect in the stimulated area and form a circular spot with high density. This mechanism of stream formation is associated with the fact that the velocity of the cAMP waves depends on the local density of the amoebae.

The reaction-diffusion model proposed describes fairly well the aggregation process in natural population of Dd. The aggregation pattern obtained by numerical simulation looks similar to the pattern in amoebae populations (Figure 2).

In addition, the technical features which makes Dd amoebae attractive as a model includes [9]:

(a) the cells exist as a homogeneous population in culture,

(b) they can be induced by physiologic stimuli to undergo normal morphogenesis in vitro thus permitting direct observation of the role of chemotaxis in organogenesis,

(c) cells can be grown in suspension culture to high density to generate kilogram quantities of material for biochemical analysis,

(d) amoeboid cells are haploid and are readily manipulated by molecular genetic techniques and

(e) the physiological response to chemotactic stimulation is synchronous in a cell population and can, therefore, be correlated with biochemical measurements.

The movement of cells can also be affected by morphogen concentrations, for example, by the chemotactic mechanism. These possibilities have recently been explored in studies combining mathematical modelling and experiments [4]. There are instances where chemotaxis is favoured as compared to other mechanism. As an example, experimental observations and interpretations of the mechanisms of cell movement during gastrulation in the chick embryo are controversial: some indicate that cells move by cellular intercalation mechanism while others point out to the chemotactic mechanism. We feel that the general reasoning would be in favour of chemotactic mechanism: the mechanism can explain the formation of compact group of moving cells represented by the Hensen's node or stem zone, while formation of such groups due to cellular interaction is problematic, if not possible. This reasoning can also be applied to other processes involving movement of compact group of cells, for example, the movement of the *Drosophila follicle cells* [5].

The analysis of morphogen gradient dynamics which is associated with the moving group of cells was done in [4]. The simplest scenario to consider is when the cells forming the moving group transcribe a gene which is not transcribed in the surrounding tissue. Then this group of cells (which will be referred to as the domain of transcription, DOT), can be represented mathematically by a segment of line (of length a) which is also moving, say, to the right.

If V represent the concentration of the transcribed mRNA, then , in the simplest case, $V = 1$ inside the DOT and $V = 0$ outside the DOT. (mRNA is a molecule of RNA that encodes a chemical "blueprint" for a protein product. It is transcribed from a DNA template and carries coding information to the sites of protein synthesis. It is held at constant concentration within cells and do not permeate through cell membranes). Furthermore, we assume that the protein, A, which is associated with the transcribed gene and produced inside the DOT can diffuse into surrounding tissue and degrade. The concentration profile, $U(x)$, of the protein is stationary from the perspective of the moving DOT (i.e. in the moving frame of reference) and satisfies the following equation:

$$D\frac{d^2U}{dx^2} - c\frac{dU}{dx} + k_1V - k_2U = 0; \qquad U(x = \pm\infty), \tag{2}$$

where

$$V = \begin{cases} 1 & \text{for} \quad 0 \leq x \leq a, \\ 0 & \text{for} \quad x > a, \\ e^{-\frac{k_1}{c}x} & \text{for} \quad x < 0. \end{cases}$$

Here D is the protein's diffusion coefficient, c is the speed of the DOT movement and k_1 and k_2 define the production and decaying rates of the protein respectively.

The plot of equation (2) solution is shown in Figure 3A; it makes an asymmetric gradient with maximum shifted back of the moving DOT and the long "tail" following the DOT. The shape of the gradient indicates that the considered protein can explain the movement of DOT provided that the cells forming the DOT are chemotactically repelled by this protein. Indeed, the concentration of protein is lower on the front border of the DOT than on its back and if the protein acts as a chemorepellent on cells composing the DOT, then the net repulsion could keep the DOT moving to the right. This hypothesis was checked in simulations on Cellular Potts model [1] which is recently one of the most popular models for simulation of biological tissues.

Analysis of the chemotactic scenarios of cell movement indicates that they always came in pairs. This means that if a certain movement pattern can be explained by the chemotaxis, then it will have at least two explanations. For example, from above, the DOT can move because the cells composing the DOT produce a self-repellent. The counterpart explanation is the following: the DOT will show the same movement pattern if the cells composing surrounding tissue produce a protein which acts as chemoattractant to the cells forming the DOT. Besides, a movement pattern can have more explanations if more cell types are involved.

Chemotaxis indeed has mathematically been studied by many authors such as Keller and Segel and it is the basis of this dissertation that I will be discussing about chemotaxis; developing computational techniques to model migration of cells. I will be looking at the movement of self repelling group of cells. The detailed analysis of the interplay of morphogen gradient and cell movement will be the focus of my dissertation and will be discussed in the preceding sections.

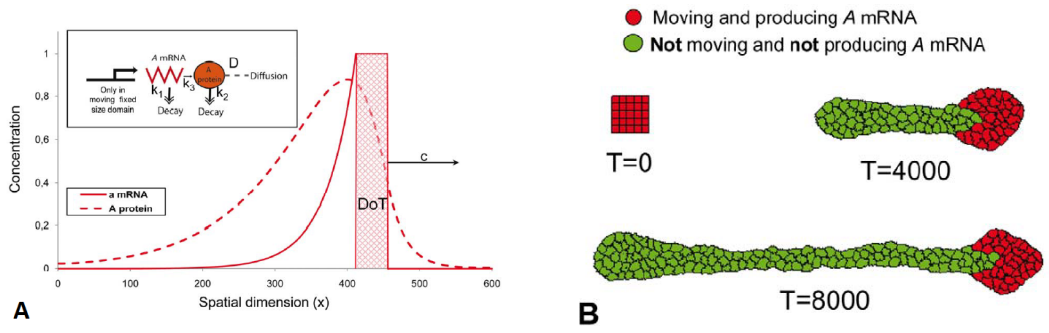

Figure 3: Group of self-repelling cells moving in (A) continuous 1-D model and (B) individual cell-based 2D model (Cellular Potts model).
In A, the solid red line denotes the concentration of A-mRNA while the dashed red line denotes the concentration of protein A. A-mRNA is produced in the DOT (it has a preset size and moves to the right with speed c. B shows three consecutive images from the simulation of primitive streak regression. Initially the group of red cells (DOT) form a square tissue. They then move (to the right), proliferate and differentiate, i.e. red cell transforms into the green cell when the level of protein A at any point inside the red cell gets above the threshold value. Green cells do not move or produce A-mRNA and for simplicity, it was assumed that they also do not proliferate.

2 Basic Model (1-D)

A group of cells that are producing chemicals and reacting to it is considered in this model. A **1-variable** reaction-diffusion system is used and the solutions arising from solving this system will be non-linear and describes the chemotaxis function.

As mentioned in the introduction, we will call a group of cells which transcribe a gene a **domain of transcription (DOT)**. A DOT can be isolated or located in the tissue; surrounded by other cells which do not transcribe a considered gene. To simplify and ease our problem, we will represent the DOT by a line segment of width a (we use the range $-\frac{a}{2} \leq x \leq \frac{a}{2}$). The DOT is then characterized by the translation of the gene and production of an extracellular diffusing protein, that acts as the chemotactic chemical. The description of this model is different from the one mentioned in the introduction.

2.1 Equation for concentration of morphogens

We have an equation describing the dynamics of the concentration of corresponding protein denoted by U. If the DOT is moving, the concentration profile of U (in a frame of reference moving with the DOT) is given by the equation

$$\frac{\partial U}{\partial t} = D\frac{d^2U}{dx^2} - k_1 U + P(x,t). \tag{3}$$

where

$$P(x,t) = \begin{cases} 1, & |x - ct| < \frac{a}{2} \ , \\ 0, & \text{otherwise} \end{cases}$$

and

D : diffusion constant,

k_1 : rate of protein decay,

P : production term.

This equation is derived using the wave equation,

$$\dot{U}(x,t) = D\frac{\partial^2 U}{\partial x^2} - k_1 U + P(x,t),$$

where $x \in (-\infty, \infty)$, $t \in [0, \infty)$.

We introduce coordinate ξ relative to wave. i.e.

$$\xi \quad = \quad x - ct.$$

which then gives us the travelling wave solution

$$U(x,t) = U(x-ct) = U(\xi).$$

Its derivative with respect to t is

$$\left.\frac{\partial U}{\partial t}\right|_{\xi} = \frac{dU}{d\xi}\frac{\partial \xi}{\partial t} = -c\frac{dU}{d\xi}$$

and with respect to x is

$$\left.\frac{\partial U}{\partial x}\right|_{\xi} = \frac{dU}{d\xi}\frac{\partial \xi}{\partial x} = \frac{dU}{d\xi}.$$

$$\Rightarrow \frac{\partial^2 U}{\partial x^2} = \frac{d^2U}{d\xi^2}.$$

Substituting these derivatives then leads to the ODE for x in terms of ξ. i.e.

$$D\frac{d^2U}{d\xi^2} + c\frac{dU}{d\xi} - k_1 U + P(\xi) = 0,$$

where

$$P(\xi) = \begin{cases} k_2 & \text{if} \quad |\xi| < -\frac{a}{2}, \\ 0 & \text{if} \quad |\xi| > \frac{a}{2}. \end{cases}$$

This gives us the equation in (3).

Since we are in a moving frame of reference, returning back to our notation in x, we will then have

$$D\frac{d^2U}{dx^2} + c\frac{dU}{dx} - k_1 U + P(x,t) \quad = \quad 0, \tag{4}$$

where

$$P(x,t) = \begin{cases} k_2 & \text{if } |x| < -\frac{a}{2}, \\ 0 & \text{if } |x| > \frac{a}{2} \end{cases}$$

and

k_2 : rate of protein production.

(We take a, D, k_1 and $k_2 \in \mathbb{R}^+$).

2.1.1 Finding the solution

Green's function is used to solve the non-linear differential equation in (4) [11].

Auxiliary equation:

$$D\lambda^2 + c\lambda - k_1 = 0,$$

$$\Rightarrow \lambda = \frac{-c \pm \sqrt{c^2 + 4k_1 D}}{2D}.$$

We denote the solutions as:

$$\lambda_1 = \frac{-c + \sqrt{c^2 + 4k_1 D}}{2D} \quad , \quad \lambda_2 = \frac{-c - \sqrt{c^2 + 4k_1 D}}{2D}. \tag{5}$$

Dividing (4) throughout by D:

$$\frac{d^2U}{dx^2} + \frac{c}{D}\frac{dU}{dx} - \frac{k_1}{D}U + \frac{k_2}{D}V = 0. \tag{6}$$

Let $U = e^{-\frac{c}{2D}x}w$. Then

$$U' = -\frac{c}{2D}e^{-\frac{c}{2D}x}w + e^{-\frac{c}{2D}x}w,$$

$$U'' = \Big(\frac{c}{2D}\Big)^2 e^{-\frac{c}{2D}x}w - \frac{c}{D}e^{-\frac{c}{2D}x}w' + e^{-\frac{c}{2D}x}w''.$$

Substituting into (6) and simplifying by dividing throughout by $e^{-\frac{c}{2D}x}$, we obtain

$$w'' - w\Big(\frac{c^2}{4D^2} + \frac{k_1}{D}\Big) = -\frac{k_2}{D}e^{\frac{c}{2D}x}V. \tag{7}$$

Green's function for (7) is:

$$G(x,y) = \frac{1}{2\chi}e^{-\chi|x-y|} \quad , \quad \chi = \frac{\sqrt{c^2 + 4k_1 D}}{2D}.$$

$$G'(x,y) = -\chi \text{sign}(x-y)\frac{1}{2\chi}e^{-\chi|x-y|} = \text{sign}(x-y)\chi G(x,y),$$

$$G''(x,y) = -\chi^2 G(x-y) - \chi\delta(x-y)G(x,y).$$

Substituting into (7):

$$G''(x,y) - \Big(\frac{c^2}{4D^2} + \frac{k_1}{D}\Big)G(x-y) = \delta(x-y).$$

We can then write

$$w(x) = \int_{-\infty}^{\infty} G(x,y)\Big(\frac{k_2}{D}e^{\frac{c}{2D}x}V\Big)dy$$

or

$$\begin{aligned} U(x) &= \int_{-\infty}^{\infty} G(x,y)\Big(\frac{k_2}{D}e^{\frac{c}{2D}y}e^{-\frac{c}{2D}x}V\Big)dy \\ &= \int_{-\infty}^{\infty} G(x,y)\Big(\frac{k_2}{D}e^{\frac{c(y-x)}{2D}}V\Big)dy \end{aligned}$$

$$\begin{aligned} \Rightarrow U(x) &= \int_{-\infty}^{\infty} \frac{1}{2\chi}e^{-\chi|x-y|}\frac{k_2}{D}e^{\frac{c(y-x)}{2D}}\,dy \\ &= \int_{-\infty}^{\infty} \frac{k_2}{\sqrt{c^2+4k_1D}}e^{\frac{-\sqrt{c^2+4k_1D}}{2D}|x-y|+\frac{c(y-x)}{2D}}V\,dy \\ &= \frac{k_2}{\sqrt{c^2+4k_1D}}\int_{-\infty}^{\infty} e^{\frac{-\sqrt{c^2+4k_1D}}{2D}|x-y|+\frac{c(y-x)}{2D}}V\,dy \\ &= \frac{k_2}{\sqrt{c^2+4k_1D}}(I_1+I_2). \end{aligned}$$

Denoting $A = e^{\frac{-\sqrt{c^2+4k_1D}}{2D}|x-y|+\frac{c(y-x)}{2D}}V$, we have

(a) for $x < -\frac{a}{2}$:

$$I_1 = \int_{-\infty}^{-\frac{a}{2}} A\;dy = 0,$$

(since $V = 0$ for $x < -\frac{a}{2}$)

$$\begin{aligned} I_2 &= \int_{-\frac{a}{2}}^{\frac{a}{2}} A\ dy \\ &= \int_{-\frac{a}{2}}^{\frac{a}{2}} e^{\frac{-\sqrt{c^2+4k_1D}+c}{2D}y+\frac{\sqrt{c^2+4k_1D}-c}{2D}x}\, dy. \end{aligned}$$

Using (5), we obtain

$$\begin{aligned} I_2 &= \int_{-\frac{a}{2}}^{\frac{a}{2}} A\ dy \\ &= \int_{-\frac{a}{2}}^{\frac{a}{2}} e^{-\lambda_1 y+\lambda_1 x}\ dy \\ &= e^{\lambda_1 x}\int_{-\frac{a}{2}}^{\frac{a}{2}} e^{-\lambda_1 y}\ dy \\ &= -\frac{e^{\lambda_1 x}}{\lambda_1}\Big(e^{-\frac{a}{2}\lambda_1}-e^{\frac{a}{2}\lambda_1}\Big) \end{aligned}$$

$$\Rightarrow U_1 = \frac{k_2}{\lambda_1\sqrt{c^2+4k_1D}}\Big(e^{(x+\frac{a}{2})\lambda_1}-e^{(x-\frac{a}{2})\lambda_1}\Big).$$

From (5),

$$\begin{aligned} \lambda_1-\lambda_2 &= \frac{\sqrt{c^2+4k_1D}}{D} \\ \Rightarrow D(\lambda_1-\lambda_2) &= \sqrt{c^2+4k_1D}. \end{aligned} \tag{8}$$

Hence

$$\begin{aligned} U_1 &= -\frac{k_2\lambda_1\lambda_2}{k_1\lambda_1(\lambda_1-\lambda_2)}\Big(e^{(x+\frac{a}{2})\lambda_1}-e^{(x-\frac{a}{2})\lambda_1}\Big) \\ &= \frac{k_2\lambda_2}{k_1(\lambda_1-\lambda_2)}\Big(e^{(x-\frac{a}{2})\lambda_1}-e^{(x+\frac{a}{2})\lambda_1}\Big). \end{aligned}$$

(b) for $-\frac{a}{2} < x < \frac{a}{2}$:

$$I_1 = \int_{-\infty}^{-\frac{a}{2}} A\ dy = 0,$$

(since $V = 0$ for $x < -\frac{a}{2}$)

$$\begin{aligned} I_2 &= \int_{-\frac{a}{2}}^{\frac{a}{2}} A\ dy \\ &= \int_{-\frac{a}{2}}^{x} e^{\frac{-\sqrt{c^2+4k_1D}}{2D}(x-y)+\frac{c}{2D}(y-x)}\ dy + \int_{x}^{\frac{a}{2}} e^{\frac{-\sqrt{c^2+4k_1D}}{2D}(y-x)+\frac{c}{2D}(y-x)}\ dy \\ &= \int_{-\frac{a}{2}}^{x} e^{-\lambda_2 y+\lambda_2 x}\ dy + \int_{x}^{\frac{a}{2}} e^{-\lambda_1 y+\lambda_1 x}\ dy \\ &= \frac{e^{\lambda_2 x}}{\lambda_2}\Big(e^{\frac{a}{2}\lambda_2} - e^{-x\lambda_2}\Big) - \frac{e^{\lambda_1 x}}{\lambda_1}\Big(e^{-\frac{a}{2}\lambda_1} - e^{-x\lambda_1}\Big). \end{aligned}$$

Hence

$$\begin{aligned} U_2 &= \frac{k_2}{\sqrt{c^2+4k_1D}}\Big\{\frac{1}{\lambda_2}\Big(e^{(x+\frac{a}{2})\lambda_2} - 1\Big) - \frac{1}{\lambda_1}\Big(e^{(x-\frac{a}{2})\lambda_1} - 1\Big)\Big\} \\ &= \frac{k_2}{\lambda_2\lambda_1\sqrt{c^2+4k_1D}}\Big(\lambda_1 e^{(x+\frac{a}{2})\lambda_2} - \lambda_2 e^{(x-\frac{a}{2})\lambda_1} - \lambda_1 + \lambda_2\Big) \\ &= \frac{k_2}{k_1(\lambda_1-\lambda_2)}\Big(\lambda_2 e^{(x-\frac{a}{2})\lambda_1} - \lambda_1 e^{(x+\frac{a}{2})\lambda_2} + \lambda_1 - \lambda_2\Big). \end{aligned}$$

(c) for $x > \frac{a}{2}$:

$$I_1 = \int_{-\infty}^{-\frac{a}{2}} A\ dy = 0,$$

(since $V = 0$ for $x < -\frac{a}{2}$)

$$\begin{aligned} I_2 &= \int_{-\frac{a}{2}}^{\frac{a}{2}} A\ dy \\ &= \int_{-\frac{a}{2}}^{\frac{a}{2}} e^{-\frac{\sqrt{c^2+4k_1D}+c}{2D}(x-y)+\frac{c}{D}(y-x)}\ dy \\ &= \int_{-\frac{a}{2}}^{\frac{a}{2}} e^{-\lambda_2 y+\lambda_2 x}\ dy \\ &= \frac{e^{\lambda_2 x}}{\lambda_2}\Big(e^{\frac{a}{2}\lambda_2} - e^{-\frac{a}{2}\lambda_2}\Big). \end{aligned}$$

Hence

$$\begin{aligned} U_3 &= \frac{k_2}{\sqrt{c^2+4k_1D}}\Big(e^{(x+\frac{a}{2})\lambda_2} - e^{(x-\frac{a}{2})\lambda_2}\Big) \\ &= \frac{k_2\lambda_1}{k_1(\lambda_1-\lambda_2)}\Big(e^{(x-\frac{a}{2})\lambda_2} - e^{(x+\frac{a}{2})\lambda_2}\Big). \end{aligned}$$

Summarising,

$$U_1 = \frac{k_2\lambda_2}{k_1(\lambda_1-\lambda_2)}\Big(e^{(x-\frac{a}{2})\lambda_1} - e^{(x+\frac{a}{2})\lambda_1}\Big). \tag{9}$$

$$U_2 = \frac{k_2}{k_1(\lambda_1-\lambda_2)}\Big(\lambda_2 e^{(x-\frac{a}{2})\lambda_1} - \lambda_1 e^{(x+\frac{a}{2})\lambda_2} + \lambda_1 - \lambda_2\Big). \tag{10}$$

$$U_3 = \frac{k_2\lambda_1}{k_1(\lambda_1-\lambda_2)}\Big(e^{(x-\frac{a}{2})\lambda_2} - e^{(x+\frac{a}{2})\lambda_2}\Big). \tag{11}$$

or

$$U = \begin{cases} \frac{k_2\lambda_2}{k_1(\lambda_1-\lambda_2)}\Big(e^{(x-\frac{a}{2})\lambda_1} - e^{(x+\frac{a}{2})\lambda_1}\Big) & \text{if} \quad x \le -\frac{a}{2}, \\ \frac{k_2}{k_1(\lambda_1-\lambda_2)}\Big(\lambda_2 e^{(x-\frac{a}{2})\lambda_1} - \lambda_1 e^{(x+\frac{a}{2})\lambda_2} + \lambda_1 - \lambda_2\Big) & \text{if} \quad -\frac{a}{2} \le x \le \frac{a}{2}, \\ \frac{k_2\lambda_1}{k_1(\lambda_1-\lambda_2)}\Big(e^{(x-\frac{a}{2})\lambda_2} - e^{(x+\frac{a}{2})\lambda_2}\Big) & \text{if} \quad x \ge \frac{a}{2}. \end{cases}$$

In obtaining these unique solutions, the following 6 boundary conditions were taken into account (the solutions must have continuous 1st derivative) :

$$\begin{array}{c|c} U_1\big(-\frac{a}{2}\big) = U_2\big(-\frac{a}{2}\big) & U_2\big(\frac{a}{2}\big) = U_3\big(\frac{a}{2}\big) \\ \frac{dU_1}{dx}\big(-\frac{a}{2}\big) = \frac{dU_2}{dx}\big(-\frac{a}{2}\big) & \frac{dU_2}{dx}\big(\frac{a}{2}\big) = \frac{dU_3}{dx}\big(\frac{a}{2}\big) \\ U_1(-\infty) = 0 & U_3(\infty) = 0 \end{array}$$

Further, the solutions obtained are not analytic since the function P in equation (4) is not analytic. (To check that P is not analytic, we can find the 2nd derivative and see if it exists. If $U_1 = U_3$, then it is continuous and the 2nd derivative exists. Otherwise it is discontinuous). Here, we will see that the 2nd derivative does not exist thus implying that P is not analytic. Hence the solutions are not analytic too (computations for the 2nd derivative is omitted here) .

2.1.2 Analysis of the concentration profile

Next, we look at what happen to the solutions for U when the parameter, c, is varied since they depend on c, which is the speed. We will analyse for the case of a stationary DOT (i.e. $c = 0$) and a moving DOT (i.e. $c \neq 0$). We then plot the concentration profiles respectively .

(a) For $c = 0$, we have a symmetric normal distribution graph as shown in Figure 4.

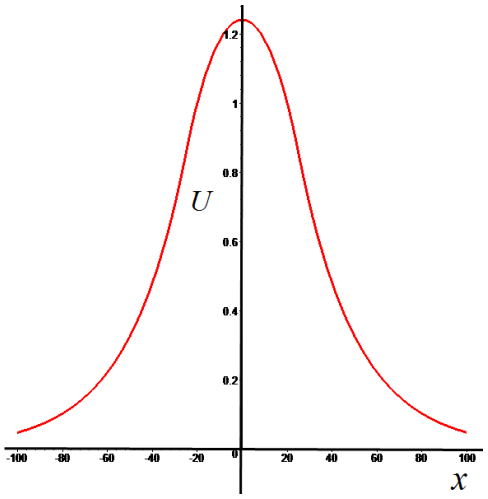

Figure 4: Profile of U for the stationary DOT (c=0).

(b) For $c \neq 0$, the graph is shown in Figure 5.

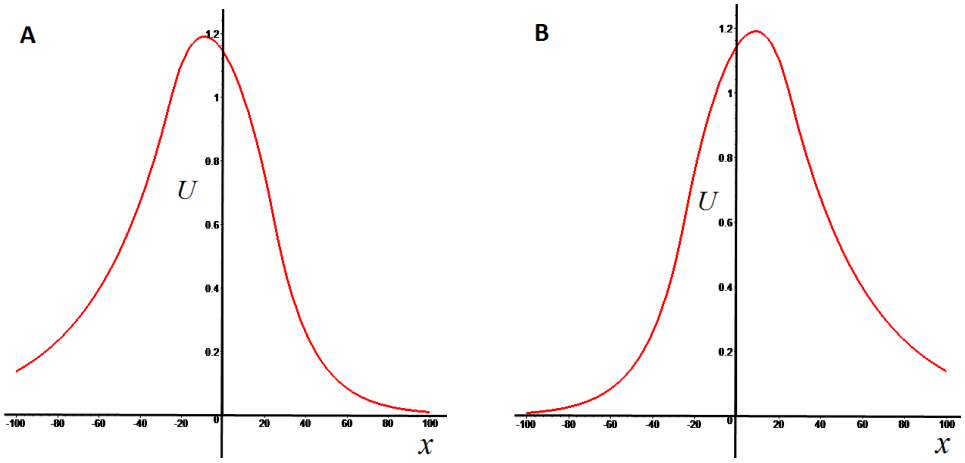

Figure 5: Concentration profiles for A: $c > 0$ and B: $c < 0$.

2.1.3 Location of maximum concentration of U

We then analyse the location at which the concentration of U is maximal. We denote it by $x_{\max}$. From Figure 4, for the case $c = 0$, it is evident that $x_{\max} = 0$ (or the origin) since we have a symmetric distribution. However, for $c \neq 0$, to locate $x_{\max}$, we will solve $\frac{dU_2}{dx} = 0$.

$$\begin{aligned}
\frac{dU_2}{dx} &= \frac{d}{dx}\Big[\frac{k_2}{k_1(\lambda_1-\lambda_2)}\Big(\lambda_2 e^{(x-\frac{a}{2})\lambda_1} - \lambda_1 e^{(x+\frac{a}{2})\lambda_2} + \lambda_1 - \lambda_2\Big)\Big] \\
&= \frac{k_2}{k_1(\lambda_1-\lambda_2)}\Big(\lambda_1\lambda_2 e^{(x-\frac{a}{2})\lambda_1} - \lambda_1\lambda_2 e^{(x+\frac{a}{2})\lambda_2}\Big) \\
&= \frac{k_2\lambda_1\lambda_2}{k_1(\lambda_1-\lambda_2)}\Big(e^{(x-\frac{a}{2})\lambda_1} - e^{(x+\frac{a}{2})\lambda_2}\Big).
\end{aligned}$$

$\frac{dU_2}{dx} = 0 \quad \Rightarrow$

$$\begin{aligned}
e^{(x-\frac{a}{2})\lambda_1} &= e^{(x+\frac{a}{2})\lambda_2} \\
e^{(x-\frac{a}{2})\lambda_1-(x+\frac{a}{2})\lambda_2} &= 1 \\
\Big(x-\frac{a}{2}\Big)\lambda_1 - \Big(x+\frac{a}{2}\Big)\lambda_2 &= 0 \\
x(\lambda_1-\lambda_2) &= \frac{a}{2}(\lambda_1+\lambda_2) \\
x_{\max} &= \frac{a}{2}\Big(\frac{\lambda_1+\lambda_2}{\lambda_1-\lambda_2}\Big).
\end{aligned}$$

Substituting equation (8) and $\lambda_1 + \lambda_2 = -\frac{c}{d}$ from equation (5) we get,

$$x_{\max} = -\frac{ac}{2\sqrt{c^2+4k_1D}}. \tag{12}$$

Figure 6 shows how the location of the maximum concentration ($x_{\max}$) changes with c.

We see that for $c > 0$, $x_{\max}$ shifts to the left, as shown in Figure 5A and for $c < 0$, $x_{\max}$ shifts to the right, as shown in Figure 5B. Equation (12) indicates that $x_{\max}$ decreases ($\to -\frac{a}{2}$) when c increases ($c > 0$). Likewise for $c < 0$ ($c \to -\infty$), $x_{\max} \to \frac{a}{2}$. $x_{\max}$ will not go beyond the range $-\frac{a}{2} \leq x \leq \frac{a}{2}$. This is because of the value of $U_{\max}$ (the computation for $U_{\max}$ is omitted here) which is again due to the function P in equation (4). In the region $x < -\frac{a}{2}$ and $x > \frac{a}{2}$, $P = 0$ (no production). Therefore

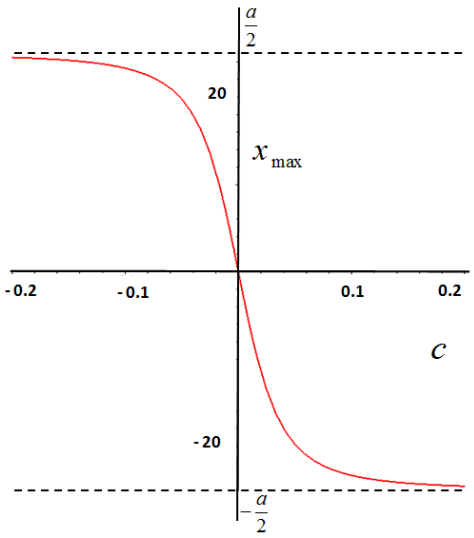

Figure 6: Location of the maximum of U versus speed, c.

$$D\frac{d^2U}{d\xi^2} + c\frac{dU}{d\xi} - k_1 U = 0.$$

This implies that we will not have a maximum. Hence due to convection, $x_{\max}$ is within $\big[-\frac{a}{2}, \frac{a}{2}\big]$.

Further, we can also conclude that

$$c \to \infty \Rightarrow U_{\max} \to 0.$$

Although we do not compute $U_{\max}$, we can show that it indeed tends to 0 when $c \to \infty$ by looking at $U(-\frac{a}{2})$. We have

$$\Delta U = U\big(-\frac{a}{2}\big) - U\big(\frac{a}{2}\big),$$

where

$$U\big(-\frac{a}{2}\big) = \frac{k_2\lambda_2}{k_1(\lambda_1 - \lambda_2)}\Big(e^{-a\lambda_1} - 1\Big). \tag{13}$$

Using the Taylor's series

$$c\sqrt{1 + \frac{4k_1\,D}{c^2}} \;=\; c\Big(1 + \frac{2k_1\,D}{c^2}\Big)$$

and substituting into equation (5), we obtain

$$\lambda_1 = \frac{k_1}{c} \quad , \quad \lambda_2 = -\frac{c}{D} - \frac{k_1}{c},$$

$$\lambda_1 - \lambda_2 = \frac{c}{D} + \frac{2\,k_1}{c} \quad , \quad e^{-a\lambda_1} = 1 - \frac{a\,k_1}{c}.$$

Now, if we substitute into equation (13) and simplifying, we obtain

$$U\big(-\frac{a}{2}\big) = \frac{k_2(ac^2k_1 + ak_1^2D)}{k_1c(2k_1D + c^2)}.$$

Applying **L'Hôpital's** rule twice, we get

$$U\big(-\frac{a}{2}\big) = \frac{2k_2k_1a}{6k_1c}$$

and finally applying **L'Hôpital's** one last time, we will get

$$U\big(-\frac{a}{2}\big) = 0.$$

$U\,(-\frac{a}{2}) > U\,(\frac{a}{2}) > 0$. Since $U\,(-\frac{a}{2}) \to 0$, this implies that $U\,(\frac{a}{2}) \to 0$. Hence $\Delta U \to 0$. Further,

$$U_{\max} \to U\,(-\frac{a}{2}) \quad \text{and} \quad \Delta U \leq U_{\max}.$$

Hence

$$U_{\max} \to 0.$$

2.1.4 Analysis of ΔU - the difference between concentration of the front and back of moving segment

The line segment (i.e. the DOT) moves due to the chemotactic response to the protein. In other words, chemotaxis is a motion due to the difference in the levels of U. i.e.

$$\Delta U \;\; = \;\; U\,\big(\frac{a}{2}\big) - U\,\big(-\frac{a}{2}\big).$$

After substituting the values of $U\,(\frac{a}{2})$ and $U\,(-\frac{a}{2})$ from the travelling solutions in equation (9) and equation (11) respectively, we obtain

$$\Delta U(c) \quad = \quad \frac{k_2}{k_1(\lambda_1 - \lambda_2)}\Big[\lambda_1(1 - e^{a\lambda_2}) + \lambda_2(1 - e^{-a\lambda_1})\Big]. \tag{14}$$

Further, the analysis of ΔU gives us:

(a) $\Delta U = 0$ when $c = 0$,

(b) when $c \to 0$, $\Delta U \to 0$. Likewise, when c increases ($c \to \infty$), $\Delta U \to 0$. This is because looking at equation (5), we will have

$$\begin{cases} \lambda_1 \to 0 & \text{as } c \to \infty, \\ \lambda_2 \to \infty & \text{as } c \to \infty, \end{cases}$$

and substituting into equation (14), we have $\Delta U \to 0$. This is further corroborated by Figure 7.

(c) $\Delta U > 0, \ \forall c > 0$,

(d) $\Delta U(c)$ has only 1 maximum.

For (d), it is not in the scope of this dissertation to prove it.

2.2 Motion due to chemotaxis

In chemotaxis, chemicals are produced either within a group of cells (internal) or by the surrounding environment (external). The cells then move with constant, uniform velocity either against (repel) or with (attract) the chemical gradient. In this section, I will be deriving conditions for this group of cells to move, given an applied force, which is the chemotaxis.

c is the difference between the front and back segment. In obtaining the expression for c, there are two considerations, one factoring the size of the DOT, a, and one which ignores a. We can derive c for both considerations by using the formula for force, $F = \text{mass} \times \text{acceleration}$.

Speed of motion is proportional to ΔU and for the existence of a wave solution, acceleration $= 0$ since c is uniform velocity. i.e. $\frac{dc}{dt} = 0$. Let

$$F_{\text{friction}} = -K_{\text{friction}} \cdot c,$$

where K_{friction} is a constant. Then

$$0 = ma = \sum F = F_{\text{friction}} + F_{\text{chemotaxis}}.$$

$$\Rightarrow F_{\text{friction}} \quad = \quad -F_{\text{chemotaxis}}.$$

We can define chemotaxis as

(a) $d\,F_{\text{chemotaxis}} = K_{\text{chemotaxis}}\,dU$.

We assume every single cell produces force and the force is proportional to the chemicals on both side. We will then have

$$\begin{aligned}
F_{\text{chemotaxis}} &= K_{\text{chemotaxis}} \int_{-\frac{a}{2}}^{\frac{a}{2}} dU \\
F_{\text{chemotaxis}} &= K_{\text{chemotaxis}} \cdot \Delta U \\
-F_{\text{friction}} &= K_{\text{chemotaxis}} \cdot \Delta U \\
K_{\text{friction}} \cdot c &= K_{\text{chemotaxis}} \cdot \Delta U \\
c &= \frac{K_{\text{chemotaxis}}}{K_{\text{friction}}} \cdot \Delta U \\
c &= c_0 \cdot \Delta U \\
c &= c_0 \Big[U\left(\frac{a}{2}\right) - U\left(-\frac{a}{2}\right) \Big]. \qquad (15)
\end{aligned}$$

c_0 is the ratio $\frac{K_{\text{chemotaxis}}}{K_{\text{friction}}}$. It is the strength of the chemotaxis or equivalently, it is the sensitivity of the group of cells to the chemical gradient.

Therefore, substituting equation (14), we have

$$c \quad = \quad \frac{k_2 c_0}{k_1(\lambda_1 - \lambda_2)} \Big[\lambda_1(1 - e^{a\lambda_2}) + \lambda_2(1 - e^{-a\lambda_1}) \Big]. \qquad (16)$$

(b) $F_{\text{chemotaxis}} = K_{\text{chemotaxis}} \bar{\nabla} U$.

We assume the total force is proportional to the average gradient. We will then have

$$
\begin{aligned}
F_{\text{chemotaxis}} &= K_{\text{chemotaxis}} \cdot \frac{1}{a} \int_{-\frac{a}{2}}^{\frac{a}{2}} \frac{dU}{dx}\, dx \\
F_{\text{chemotaxis}} &= \frac{K_{\text{chemotaxis}}}{a} \cdot \Delta U \\
-F_{\text{friction}} &= \frac{K_{\text{chemotaxis}}}{a} \cdot \Delta U \\
K_{\text{friction}} \cdot c &= \frac{K_{\text{chemotaxis}}}{a} \cdot \Delta U \\
c &= \frac{K_{\text{chemotaxis}}}{a \cdot K_{\text{friction}}} \cdot \Delta U \\
c &= \frac{c_0}{a} \cdot \Delta U.
\end{aligned}
$$

Substituting equation (14), we obtain

$$
c = \frac{k_2 c_0}{a k_1 (\lambda_1 - \lambda_2)} \Big[\lambda_1 (1 - e^{a\lambda_2}) + \lambda_2 (1 - e^{-a\lambda_1}) \Big]. \tag{17}
$$

For consistency, in this dissertation, the calculations and results are based on equation (16). i.e. we do not consider the size of the DOT, a, in the denominator. However, for comparison, in section 3.3 of my paper, I will show the computations and results using equation (17) as well.

Now, equation (16) defines the speed of chemotactically moving segment, which is given by the points of intersection of two lines $y = c$ and $y = f(c)$ where $f(c)$ is the RHS of equation (16). It is the function responsible for motion and gives the definition of the chemotaxis function. It is a non-linear function since λ_1 and λ_2 are both functions of c. Further it is also implicit in c.

There is at least one solution when the RHS = 0 (i.e. $c = 0$), which corresponds to the stationary segment. Travelling solutions then corresponds to $c \neq 0$. Such solutions definitely exist if $f'(c) > 1$ for $c = 0$.

For $c = 0$,

$$
\lambda_1|_{c=0} = \sqrt{\frac{k_1}{D}} \quad , \quad \lambda_2|_{c=0} = -\sqrt{\frac{k_1}{D}} \quad , \quad \left.\frac{d\lambda_1}{dc}\right|_{c=0} = -\frac{1}{2D} \quad , \quad \left.\frac{d\lambda_2}{dc}\right|_{c=0} = -\frac{1}{2D}. \tag{18}
$$

$$f(c) \;=\; \frac{k_2 c_0}{k_1(\lambda_1-\lambda_2)}\Big[\lambda_1(1-e^{a\lambda_2})+\lambda_2(1-e^{-a\lambda_1})\Big].$$

Therefore

$$\begin{aligned}
f'(c) &= \frac{k_2c_0}{k_1}\frac{d}{dc}\Big[\frac{\lambda_1(1-e^{a\lambda_2})}{\lambda_1-\lambda_2}+\frac{\lambda_2(1-e^{-a\lambda_1})}{\lambda_1-\lambda_2}\Big] \\
&= \frac{k_2c_0}{k_1(\lambda_1-\lambda_2)^2}\Bigg\{(\lambda_1-\lambda_2)\Big[\frac{d\lambda_1}{dc}(1-e^{a\lambda_2})-a\frac{d\lambda_2}{dc}\lambda_1e^{a\lambda_2}\Big]-\lambda_1(1-e^{a\lambda_2})\Big(\frac{d\lambda_1}{dc}-\frac{d\lambda_2}{dc}\Big) \\
&+ (\lambda_1-\lambda_2)\Big[\frac{d\lambda_2}{dc}(1-e^{-a\lambda_1})+a\frac{d\lambda_1}{dc}\lambda_2e^{-a\lambda_1}-\lambda_2(1-e^{-a\lambda_1})\Big(\frac{d\lambda_1}{dc}-\frac{d\lambda_2}{dc}\Big)\Big]\Bigg\}.
\end{aligned}$$

Substituting (18), we then have

$$\begin{aligned}
f'(c) &= \frac{k_2c_0}{k_1}\left[-\frac{1}{2D}\Big(1-e^{-a\sqrt{\frac{k_1}{D}}}\Big)+\frac{a}{2D}\sqrt{\frac{k_1}{D}}e^{-a\sqrt{\frac{k_1}{D}}}-\frac{1}{2D}\Big(1-e^{-a\sqrt{\frac{k_1}{D}}}\Big)+\frac{a}{2D}\sqrt{\frac{k_1}{D}}e^{-a\sqrt{\frac{k_1}{D}}}\right] \\
&= \frac{k_2c_0}{k_1}\left(\frac{1}{2\sqrt{\frac{k_1}{D}}}\right)\left[-\frac{1}{D}\Big(1-e^{-a\sqrt{\frac{k_1}{D}}}\Big)+\frac{a}{D}\sqrt{\frac{k_1}{D}}e^{-a\sqrt{\frac{k_1}{D}}}\right] \\
&= \frac{k_2c_0}{2Dk_1\sqrt{\frac{k_1}{D}}}\left(e^{-a\sqrt{\frac{k_1}{D}}}-1+a\sqrt{\frac{k_1}{D}}e^{-a\sqrt{\frac{k_1}{D}}}\right) \\
&= \frac{k_2c_0}{2k_1\sqrt{k_1D}}\left[e^{-a\sqrt{\frac{k_1}{D}}}\Big(a\sqrt{\frac{k_1}{D}}+1\Big)-1\right].
\end{aligned}$$

Hence for a travelling solution to exist, we need

$$\frac{k_2c_0}{2k_1\sqrt{k_1D}}\left[e^{-a\sqrt{\frac{k_1}{D}}}\Big(a\sqrt{\frac{k_1}{D}}+1\Big)-1\right] \;>\; 1. \tag{19}$$

Figure 7 illustrates the travelling solutions for the chemotaxis function. As we can see, solutions exist for $f'(c) > 1$. (the points of intersections give the solutions). These solutions occur in pairs with opposite sign which are interpreted as chemo-attraction and chemo-repulsion. Further, we can expect that these solutions represent a group moving with constant and uniform speed.

To further analyse this plot and for a further possible point of discussion, for c

positive, i.e. the region $c \in [0, \infty)$, how do we affirm there is exactly 1 maximum? Why can't there be more than 1? Or can we have no maximum at all? Can we have instead of Figure 7, a diagram which looks like Figure 8?

One way to look at it, which is very tedious, is to find the 2^{nd} derivative of $f(c)$ (very cumbersome!). If it is always negative, then we will have one maximum point. Also, having multiple maximums may lead to different problems arising compared to the absence of a maximum. However it is not in the scope of this paper for it to be discussed.

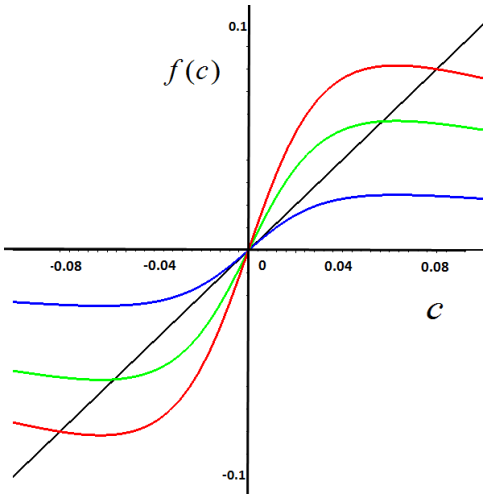

Figure 7: Plot of $f(c)$ vs c for different c_0 using Maple. Red: $c_0 = -10$, Green: $c_0 = -7$, Blue: $c_0 = -3$. Travelling solutions exist for small c_0 but not otherwise.

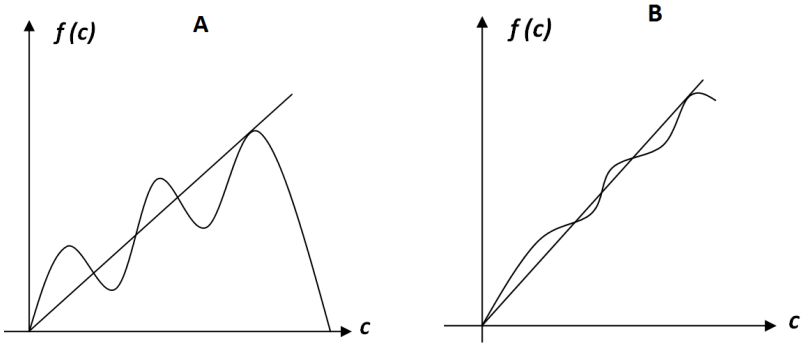

Figure 8: Plot of $f(c)$ vs c. Two other possibilities may occur, either obtaining multiple maximum points (A) or no maximum point (B).

3 Analysis of the basic model

In equation (16), we have 5 parameters, namely c_0, a, D, k_1, k_2. I will investigate how varying these model parameters will affect the velocity and thus analyse its implications.

3.1 Varying $k_2\, c_0$

$k_2\, c_0$ is a product of k_2 and c_0. It then follows that the analysis for k_2 and c_0 respectively will be the same as the analysis of $k_2\, c_0$ as they are simply proportional.

From equation (16), we can see that the chemotaxis function is an odd function. i.e. a function $f(x)$ is odd if $f(-x) = -f(x)$. Therefore we can expect two, instead of one solution to exist, which are equal in magnitude but opposite in sign. These solutions are represented by Figure 5A and Figure 5B, for attraction and repulsion respectively.

To determine the magnitude of the solutions (i.e. the chemotactic response of the group given as a velocity c) and if the group is attracted or repelled, we will look at the magnitude and sign of $k_2 c_0$, where c_0 represents the sensitivity of chemotaxis or the sensitivity of the group of cells to the chemical gradient. Travelling solutions will exist regardless of the sign for $k_2 c_0$ of sufficient magnitude. We will see how c depends on $k_2 c_0$. i.e. how the roots depend on $k_2 c_0$. We shall investigate which c_0 gives only 1 possible root (the stationary value) and which c_0 gives 2 further roots, giving a total of 3 roots. By rearranging equation (19) and making $k_2 c_0$ the subject of the formula, we can determine this condition.

Rearranging equation (19), we obtain:

$$k_2\, c_0 \quad > \quad \frac{2k_1\sqrt{k_1 D}}{\left[e^{-a\sqrt{\frac{k_1}{D}}}\left(a\sqrt{\frac{k_1}{D}}+1\right)-1\right]}. \tag{20}$$

Therefore, if equation (20) is satisfied, travelling solutions exist and the group of cells is either attracted or repelled. We will have a total of 3 roots. Else, we will have only 1 root (the stationary solution).

Presence of pitchfork bifurcation in the chemotaxis function

Pitchfork bifurcation occurs around non-hyperbolic equilibrium point for so-called odd functions and generally occurs in systems with symmetry. Figure 9 shows a pitchfork bifurcation.

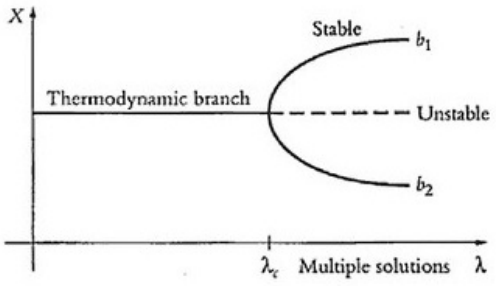

Figure 9: Pitchfork Bifurcation.

Here, concentration X is a function of λ, which measures the distance from equilibrium whereby at the bifurcation point λ_c, the branch becomes unstable and two new solutions, b_1 and b_2 emerge. We can consider a cubic equation

$$\frac{d\,c}{d\,t} = F(c, c_0) = c(c^2 + c_0).$$

If $c_0 = 0$, there will be 1 root. On the other hand, if $c_0 \neq 0$, or more accurately, $c_0 < 0$, then there will be two further roots which merges continuously from the 1^{st} root. Further, in replacing the ordinary differential equation, $F(c, c_0)$ with its Taylor series, pitchfork bifurcation takes place if

(1) $\frac{\partial f}{\partial c} = 0$,

(2) $\frac{\partial^3 f}{\partial c^3} \neq 0$,

(3) $\frac{\partial^3 f}{\partial c \partial c_0} \neq 0$.

Therefore, for our case, we have, at $c = 0$, a single stable stationary solution. Then it bifurcates at a critical value of c^*, branching into two new solutions which are equal in magnitude but opposite in sign. i.e. we obtain a pitchfork bifurcation. The plot illustrating the presence of a pitchfork bifurcation in the chemotaxis function is shown in Figure 10.

Looking back at the concentration profiles in Section 2.1.2, we see that when $c > 0$, the cells are repelled and the profile move left-wise. Vice-versa, when $c < 0$, the cells are attracted and the profile move right-wise. The positive solution, c_1, indicated in Figure 10 corresponds to repulsion of cells to the chemical while the negative solution, c_2, corresponds to attraction of cells towards the chemical gradient. (see Figure 11A and Figure 11B).

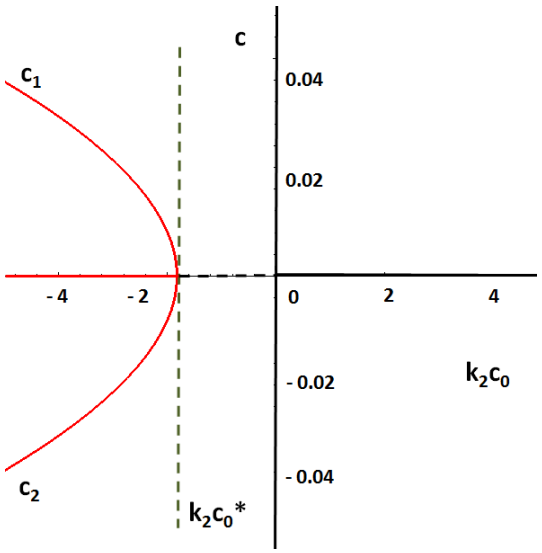

Figure 10: Plot of c vs $k_2\, c_0$ using Maple. $c \to -\infty$ when $k_2 c_0 \to -\infty$.

Further, from Figure 10, we may expect that $c \to \infty$ when $c_0 \to \infty$. How can we prove this?

Theorem: Depending on the value of the parameter c_0 , we can get the movement with any speed c.

Corollary: When $c_0 \to \infty$, $c \to \infty$.

Proof: From Figure 7, we see that, for every c_0, we can find c. i.e. we have a root for equation (16). We also have

$$c = c_0 \cdot \Delta U.$$

Let's consider the root c_1, where $c_1 > 0$. We can prove, for any c_1, there is c_0 such that $c_1 = c_0 \cdot \Delta U$.

Assume $\Delta U(c_1) = \delta$ $(\delta > 0)$ and let $c_0 = \frac{c_1}{\delta}$. Then

$$c_0 \cdot \Delta U(c_1) = \frac{c_1}{\delta}\, \delta = c_1.$$

This implies that c_1 is a root. If we increase the root c_1, c_0 will also increase. Inversely, if c_0 increases, so does c_1. i.e.

$$c_0 \to \infty \Rightarrow c_1 \to \infty.$$

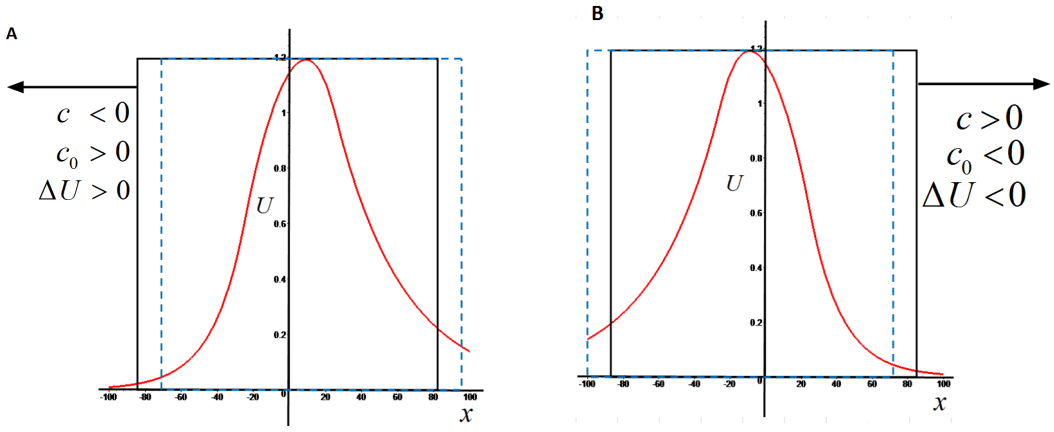

Figure 11: A: chemo-attraction, B: chemo-repulsion.

3.2 Varying k_1

Next, we analyse the effect of varying k_1, which is the rate of decay of the protein. Similar to Figure 7, Figure 12 again shows the plot of c vs $f(c)$. However, here, we have the value of k_1 varied. In Figure 12A, the red curve has a value of $k_1 = 0.045$, while the blue curve has a value of $k_1 = 0.01$. This implies that the higher the rate of decay, travelling solutions ceased to exist. We further conclude that k_1 plays an important role in the speed of the DOT migration, c. We shall investigate the relationship between k_1 and c and show it in terms of a graph.

Furthermore, from Figure 12A, we can see that the chemotaxis function, $f(c, k_1)$, tends to a certain common value as k_1 decreases. Hence, I will also be investigating, which value $f(c, k_1)$ tends to when $k_1 \to 0$ (or k_1 becomes small) as shown in Figure 12B . We let $k_1 = \epsilon$ and apply Taylor's series.

Using the Taylor's expansion

$$\sqrt{1 + \frac{4\epsilon D}{c^2}} \quad = \quad 1 + \frac{2\epsilon D}{c^2} + O\left(\epsilon^2\right).$$

and substituting into equation (5), we obtain

$$\lambda_1 = \frac{\epsilon}{c} \quad , \quad \lambda_2 = -\frac{c}{D} - \frac{\epsilon}{c} \quad , \quad \lambda_1 + \lambda_2 = -\frac{c}{D},$$

$$\lambda_1 - \lambda_2 = \frac{c}{D} + \frac{2\,\epsilon}{c} \quad , \quad e^{-a\lambda_1} = 1 - \frac{a\,\epsilon}{c}.$$

Now, if we substitute into equation (16), we obtain

$$\begin{aligned} c &= \frac{k_2 c_0}{\epsilon(\lambda_1 - \lambda_2)}\Big[\frac{\epsilon}{c}(1 - e^{a\lambda_2}) + \Big(-\frac{c}{D} - \frac{\epsilon}{c}\Big)\Big(\frac{a\,\epsilon}{c}\Big)\Big] \\ &= \frac{k_2 c_0}{k_1(\lambda_1 - \lambda_2)}\Big[\frac{\epsilon}{c} - \frac{\epsilon}{c}e^{a\lambda_2} - \frac{a\,\epsilon}{D} - \frac{a\,\epsilon^2}{c^2}\Big]. \end{aligned}$$

Then, using

$$e^{a\lambda_2} = e^{-\frac{a\,\epsilon}{c}} e^{-\frac{a\,c}{D}},$$

and omitting the quadratic term, we obtain

$$c = \frac{k_2 c_0}{\epsilon(\lambda_1 - \lambda_2)}\Big[\frac{\epsilon}{c} - \frac{\epsilon}{c}e^{-\frac{a\,\epsilon}{c}} e^{-\frac{a\,c}{D}} - \frac{a\,\epsilon}{D}\Big].$$

With a bit of manipulation, we then get

$$c = \frac{k_2 c_0}{\epsilon(\lambda_1 - \lambda_2)}\left[\frac{\frac{\epsilon}{c}e^{\frac{a\,c}{D}} - \frac{\epsilon}{c}e^{-\frac{a\,\epsilon}{c}} - \frac{a\,\epsilon}{D}e^{\frac{a\,c}{D}}}{e^{\frac{a\,c}{D}}}\right].$$

Applying the Taylor's expansion

$$e^{\frac{a\,c}{D}} = 1 + \frac{a\,c}{D},$$

we obtain

$$\begin{aligned} c &= \frac{k_2 c_0}{\epsilon(\lambda_1 - \lambda_2)}\left[\frac{\Big(1 + \frac{a\,c}{D}\Big)\Big(\frac{\epsilon}{c} - \frac{a\,\epsilon}{D}\Big) - \frac{\epsilon}{c}\Big(1 - \frac{a\,\epsilon}{c}\Big)}{1 + \frac{a\,c}{D}}\right] \\ &= \frac{k_2 c_0 D}{\epsilon(\lambda_1 - \lambda_2)}\left(-\frac{\frac{a^2\,\epsilon\,c}{D^2}}{D + a\,c}\right) \\ &= \frac{k_2\,c_0\,c\,D^2}{\epsilon(c^2 + 2\,\epsilon\,D)}\left(-\frac{\frac{a^2\,\epsilon\,c}{D^2}}{D + a\,c}\right). \end{aligned}$$

By cancellation and ignoring the term $2\,\epsilon\,D$, we finally have

$$c^* = -\frac{k_2 c_0 a^2}{D + ac}, \tag{21}$$

which gives us a quadratic equation in c. i.e.

$$cD + c^2 a + k_2 c_0 a^2 = 0.$$

Now, for example, substituting the following values: $c_0 = -10$, $k_2 = 0.0015$, $a = 10$ and $D = 0.5$, we will get

$$\begin{aligned} 0.5c + 10c^2 - 1.5 &= 0 \\ 10c^2 + 0.5c - 1.5 &= 0 \\ \Rightarrow c^* &= \frac{-0.5 \pm \sqrt{60.25}}{20} \\ &= 0.36, -0.41. \end{aligned}$$

This implies that for $k_1 \to 0$, $c = f(c)$ saturates to a value of 0.36 and -0.41. This is indeed corroborated by Figure 12B.

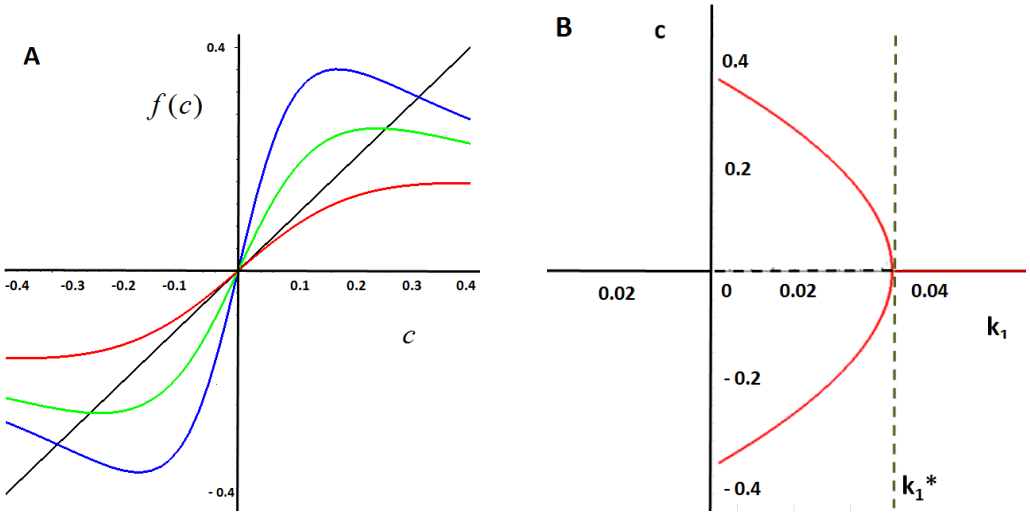

Figure 12: Plot of $f(c)$ vs c for different k_1 using Maple. A: Red: $k_1 = 0.045$, Green: $k_1 = 0.02$, Blue: $k_1 = 0.01$. Travelling solutions exist for k_1 small but not otherwise. B: Plot of c vs k_1 using Maple. The plot indicates that $c \to 0.4$ when $k_1 \to 0$. The bifurcation value of k_1 is $k_1^* = 0.04$.

We are also interested to find out the point where the solution bifurcates. We denote the point as k_1^* and let $c = \epsilon$.

First, we assume $\lambda_1\, a,\ \lambda_2\, a \ll 1$. We use the Taylor's expansion

$$\begin{aligned}\sqrt{\epsilon^2 + 4\,k_1\,D} &= 2\sqrt{k_1\,D}\sqrt{1+\frac{\epsilon^2}{4\,k_1\,D}},\\ &= 2\sqrt{k_1\,D}\Big(1+\frac{\epsilon^2}{8\,k_1\,D}\Big).\end{aligned}$$

Substituting into equation (5),

$$\lambda_1 = -\frac{\epsilon}{2D} + \sqrt{\frac{k_1}{D}} \quad , \quad \lambda_2 = -\frac{\epsilon}{2D} - \sqrt{\frac{k_1}{D}} \quad , \quad \lambda_1 - \lambda_2 = 2\sqrt{\frac{k_1}{D}}.$$

We also use 2^{nd} order approximation for the exponents. i.e.

$$\begin{aligned}e^{-a\,\lambda_1} &= 1 - a\,\lambda_1 + \frac{(a\,\lambda_1)^2}{2},\\ e^{a\,\lambda_2} &= 1 + a\,\lambda_2 + \frac{(a\,\lambda_2)^2}{2},\end{aligned}$$

Using equation (16), our computations are as follows:

$$\begin{aligned}\epsilon &= \frac{k_2 c_0}{k_1(\lambda_1-\lambda_2)}\Big[\lambda_1\Big(1-1-a\,\lambda_2-\frac{(a\,\lambda_2)^2}{2}\Big)+\lambda_2\Big(1-1+a\,\lambda_1-\frac{(a\,\lambda_1)^2}{2}\Big)\Big]\\ &= \frac{k_2 c_0}{k_1(\lambda_1-\lambda_2)}\Big[\lambda_1\Big(-a\,\lambda_2-\frac{(a\,\lambda_2)^2}{2}\Big)+\lambda_2\Big(a\,\lambda_1-\frac{(a\,\lambda_1)^2}{2}\Big)\Big]\\ &= \frac{k_2 c_0}{k_1(\lambda_1-\lambda_2)}\Big[-\frac{a^2}{2}\lambda_1\,\lambda_2(\lambda_1+\lambda_2)\Big]\\ &= \frac{k_2 c_0}{2k_1\sqrt{\frac{k_1}{D}}}\Big[-\frac{a^2}{2}\Big(-\frac{\epsilon}{D}\Big)\Big(-\frac{\epsilon}{2D}+\sqrt{\frac{k_1}{D}}\Big)\Big(-\frac{\epsilon}{2D}-\sqrt{\frac{k_1}{D}}\Big)\Big]\\ &= \frac{k_2 c_0}{2k_1\sqrt{\frac{k_1}{D}}}\Big[\frac{a^2\,\epsilon}{2\,D}\Big(\frac{\epsilon^2}{4D^2}-\frac{k_1}{D}\Big)\Big].\end{aligned}$$

Ignoring the quadratic term, we then have

$$\epsilon = \frac{k_2 c_0}{2k_1\sqrt{\frac{k_1}{D}}}\Big(-\frac{a^2\,k_1\,\epsilon}{2\,D^2}\Big).$$

Simplifying

$$\begin{aligned} 4\,D^2\sqrt{\frac{k_1}{D}} &= -k_2\,c_0\,a^2 \\ \Rightarrow k_1^* &= \frac{k_2^2\,c_0^2\,a^4}{16\,D^3}. \end{aligned} \tag{22}$$

Now, using the values: $D = 0.5$, $c_0 = -10$, $k_1 = 0.00075$ and $k_2 = 0.0015$, we get $k_1^* = 1.125$. With this value of k_1^*, substituting in $\lambda_1\,a$, we have

$$\lambda_1\,a = \sqrt{\frac{k_1}{D}}\,a = 15,$$

which is not small as assumed. So we arrived at a contradiction.

Now, let's assume $\lambda_1\,a$, $\lambda_2\,a \gg 1$. We then have

$$e^{-a\,\lambda_1} \to e^{-\infty} = 0 \quad , \quad e^{a\,\lambda_2} \to e^{-\infty} = 0.$$

So these give us

$$\begin{aligned} c &= \frac{k_2 c_0}{a k_1(\lambda_1 - \lambda_2)}(\lambda_1 + \lambda_2) \\ &= \frac{k_2\,c_0}{2\,a\,k_1\sqrt{\frac{k_1}{D}}}\Big(-\frac{c}{D}\Big) \\ 2\,a\,k_1\,\sqrt{k_1 D} &= -k_2\,c_0 \\ \Rightarrow k_1^* &= \left(\frac{k_2^2\,c_0^2}{4\,a^2\,D}\right)^{\frac{1}{3}}. \end{aligned}$$

Substituting the same values as before, we obtain

$$k_1^* = 0.01.$$

It then follows that

$$\lambda_1\,a = \sqrt{\frac{k_1}{D}}\,a = 1.4.$$

If we are to look at Figure 12B, we see that $k_1^* \approx 0.04$. Although 0.01 and 0.04 has the same order of magnitude, but $\lambda_1\,a = 1.4$ is not big enough (which is what we

assumed).

These results shows that there is no accuracy between the results obtained analytically and numerically since we arrived at a contradiction. Therefore, we will need to rely on the results obtained numerically i.e. the plot instead of analytically. Hence, our conclusion is that the bifurcation point is $k_1^* = 0.04$.

3.3 Varying a

The choice of a, i.e. the width of the DOT also affects the existence of travelling solutions. To see the implications of varying a, we shall consider both equations (16) and (17). i.e. the chemotaxis function with and without a in the denominator. From Figure 13, we see that travelling solutions exist when the width a is big but not otherwise.

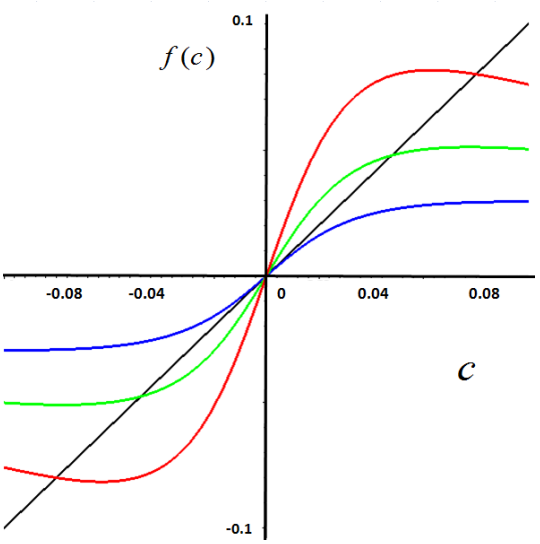

Figure 13: Plot of $f(c)$ vs c for different a using Maple. Red: $a = 10$, Green: $a = 5$, Blue: $a = 2.5$. Travelling solutions exist for large a but not otherwise.

First, we shall look at the significance of varying a using equation (17) and Figure 14 shows how c changes with a. To find out the expression for the 2 values of a^* when $c \to 0$, we again use Taylor's approximation.

For a small, i.e. $a \to 0$, we will let $c = \epsilon$. The steps are similar to finding k_1^*.

We use the following approximations for our computations.

$$\begin{aligned}\sqrt{c^2+4\,k_1\,D} &= 2\sqrt{k_1\,D}\sqrt{1+\frac{c^2}{4\,k_1\,D}},\\ &= 2\sqrt{k_1\,D}\Big(1+\frac{c^2}{8\,k_1\,D}\Big).\end{aligned}$$

Therefore, substituting into equation (5),

$$\lambda_1 = -\frac{c}{2D}+\sqrt{\frac{k_1}{D}} \quad , \quad \lambda_2 = -\frac{c}{2D}-\sqrt{\frac{k_1}{D}} \quad , \quad \lambda_1-\lambda_2 = 2\sqrt{\frac{k_1}{D}}.$$

We use 2^{nd} order approximation for the exponents. i.e.

$$\begin{aligned}e^{-a\,\lambda_1} &= 1-a\,\lambda_1+\frac{(a\,\lambda_1)^2}{2},\\ e^{a\,\lambda_2} &= 1+a\,\lambda_2+\frac{(a\,\lambda_2)^2}{2},\end{aligned}$$

Using equation (16), our computations are as follows:

$$\begin{aligned}c &= \frac{k_2c_0}{ak_1(\lambda_1-\lambda_2)}\Big[\lambda_1\Big(1-1-a\,\lambda_2-\frac{(a\,\lambda_2)^2}{2}\Big)+\lambda_2\Big(1-1+a\,\lambda_1-\frac{(a\,\lambda_1)^2}{2}\Big)\Big]\\ &= \frac{k_2c_0}{ak_1(\lambda_1-\lambda_2)}\Big[\lambda_1\Big(-a\,\lambda_2-\frac{(a\,\lambda_2)^2}{2}\Big)+\lambda_2\Big(a\,\lambda_1-\frac{(a\,\lambda_1)^2}{2}\Big)\Big]\\ &= \frac{k_2c_0}{ak_1(\lambda_1-\lambda_2)}\Big[-\frac{a^2}{2}\lambda_1\,\lambda_2(\lambda_1+\lambda_2)\Big]\\ &= \frac{k_2c_0}{2ak_1\sqrt{\frac{k_1}{D}}}\Big[-\frac{a^2}{2}\Big(-\frac{c}{D}\Big)\Big(-\frac{c}{2D}+\sqrt{\frac{k_1}{D}}\Big)\Big(-\frac{c}{2D}-\sqrt{\frac{k_1}{D}}\Big)\Big]\\ &= \frac{k_2c_0}{2ak_1\sqrt{\frac{k_1}{D}}}\Big[\frac{a^2\,c}{2\,D}\Big(\frac{c^2}{4D^2}-\frac{k_1}{D}\Big)\Big].\end{aligned}$$

Ignoring the quadratic term, since $c^2=\epsilon^2$ is very small, we then have

$$c = \frac{k_2c_0}{2ak_1\sqrt{\frac{k_1}{D}}}\Big(-\frac{a^2\,k_1\,c}{2\,D^2}\Big).$$

Simplifying

$$\begin{aligned} 1 &= -\frac{k_2\, c_0\, a}{4\, D\sqrt{k_1 D}} \\ \Rightarrow a^* &= -\frac{4\, D\sqrt{k_1 D}}{k_2\, c_0}. \end{aligned} \tag{23}$$

Now, substituting the values used previously, i.e. $D = 0.5$, $c_0 = -10$, $k_1 = 0.00075$ and $k_2 = 0.0015$, we have, when $c \to 0$ and $a \to 0$,

$$a^* = 2.58,$$

which is the value approximately shown in Figure 14A.

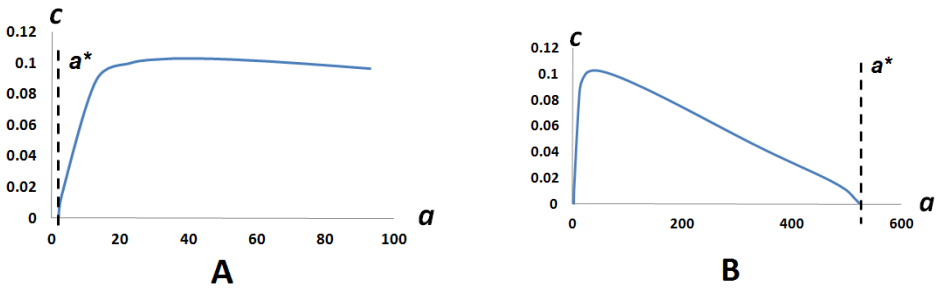

Figure 14: Plot of c vs a for equation (17) using Maple. A: $0 \le a \le 100$, B: $0 \le a \le 600$. There are two values of a when $c \to 0$.

For a big, i.e. $a \to \infty$, we will then have

$$e^{-a\,\lambda_1} \to e^{-\infty} = 0 \quad , \quad e^{a\,\lambda_2} \to e^{-\infty} = 0.$$

So this gives us

$$\begin{aligned} c &= \frac{k_2 c_0}{a k_1(\lambda_1 - \lambda_2)}(\lambda_1 + \lambda_2) \\ &= \frac{k_2\, c_0}{2\, a\, k_1 \sqrt{\frac{k_1}{D}}}\Big(-\frac{c}{D}\Big) \\ 2\, a\, k_1\, \sqrt{k_1 D} &= -k_2\, c_0 \\ \Rightarrow a^* &= -\frac{k_2\, c_0}{2\, k_1\, \sqrt{k_1 D}}\,. \end{aligned} \tag{24}$$

Substituting values, we have, when $c \to 0$ and $a \to \infty$,

$$a^* = 516.4,$$

which is indeed the value approximately shown in Figure 14B.

Now, we shall see the difference if we are to consider equation (16) instead. As shown above, for $a \to \infty$, we have both the exponents in equation (16) tending to 0. Hence we will have no a to work with. i.e. we will have no solution for a^*. So what then is the implication? Figure 15 shows the plot of c vs a using equation (16). We can see that as a increases, c will increase as well and saturates to a value close to 20.

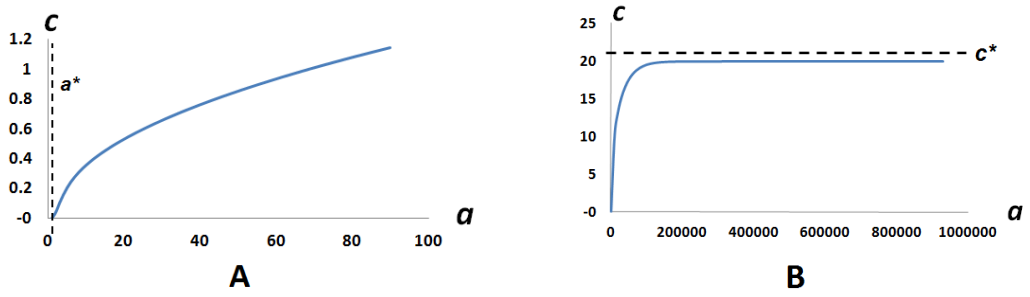

Figure 15: Plot of c vs a for equation (16) using Maple. A: $0 \leq a \leq 100$, B: $0 \leq a \leq 10^6$. c saturates to a value close to 20 as $a \to \infty$.

We shall find out what is a^* for a small and c^* for $a \to \infty$.

For $a \to 0$, equation (23) will now be:

$$\begin{aligned} 1 &= -\frac{k_2\, c_0\, a^2}{4\, D\sqrt{k_1 D}} \\ \Rightarrow a^* &= \sqrt{-\frac{4\, D\sqrt{k_1 D}}{k_2\, c_0}}. \end{aligned} \tag{25}$$

Substituting values, we have, when $a \to 0$,

$$a^* = 1.6,$$

as approximately shown in Figure 15A.

Now, for $a \to \infty$, $e^{-a\,\lambda_1} \to e^{-\infty} = 0$ and $e^{a\,\lambda_2} \to e^{-\infty} = 0$, giving us, same as before,

$$c \;=\; \frac{k_2 c_0}{a k_1(\lambda_1 - \lambda_2)}(\lambda_1 + \lambda_2).$$

The Taylor's expansion

$$\sqrt{1 + \frac{4\,k_1\,D}{c^2}} \;=\; 1 + \frac{2\,k_1\,D}{c^2} + O\left(\epsilon^2\right)$$

gives us

$$\lambda_1 = \frac{k_1}{c} \quad , \quad \lambda_2 = -\frac{c}{D} - \frac{k_1}{c} \quad , \quad \lambda_1 + \lambda_2 = -\frac{c}{D} \quad , \quad \lambda_1 - \lambda_2 = \frac{c}{D} + \frac{2\,k_1}{c}.$$

We then have

$$\begin{aligned} c &= \frac{k_2\,c_0}{k_1\left(\frac{c}{D} + \frac{2\,k_1}{c}\right)}\left(-\frac{c}{D}\right) \\ k_1\,D\left(\frac{c}{D} + \frac{2\,k_1}{c}\right) &= -k_2\,c_0 \\ c^2 + 2\,k_1 D &= -\frac{k_2\,c_0\,c}{k_1} \\ c^2 + \frac{k_2\,c_0}{k_1}\,c + 2\,k_1 D &= 0. \end{aligned}$$

Solving the quadratic equation in c and using the same values as before give us

$$c^2 - 20\,c + 0.00075 = 0.$$

We then obtain

$$c^* = 19.9$$

which is the value that is indeed corroborated by Figure 15B.

3.4 Varying D

If there is no diffusion i.e. $D = 0$, our concentration profile will simply be rectangular, as shown in Figure 16. We have $c = c_0 \cdot \Delta U$. Using equation (4), for $D \to 0$, we will have

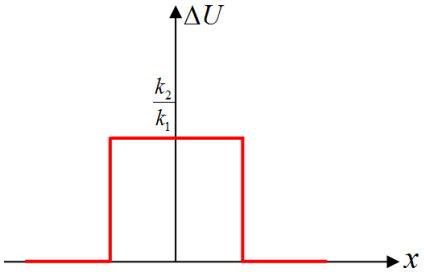

Figure 16: Concentration profile of ΔU for $D = 0$. i.e. there is no diffusion.

$$\begin{aligned} \Delta U &= \frac{k_2}{k_1} \\ \Rightarrow c^* &= c_0 \cdot \frac{k_2}{k_1}. \end{aligned} \tag{26}$$

Substituting the same values again, i.e. $c_0 = -10$, $k_1 = 0.00075$ and $k_2 = 0.0015$, we then have

$$c^* = 20.$$

If we are to compute this value analytically, we will obtain the same answer. We let $D = \epsilon$ to represent D small. In this case, Taylor's approximations give us

$$\lambda_1 = -\frac{k_1}{c} \quad , \quad \lambda_2 = -\frac{c}{\epsilon} - \frac{k_1}{c} \quad , \quad \lambda_1 - \lambda_2 = 2\frac{k_1}{c} - \frac{c}{\epsilon}.$$

Since $\epsilon \ll 1$, $\frac{c}{\epsilon}$ is big. So we can ignore the term $\frac{k_1}{c}$ in λ_2 and $\lambda_1 - \lambda_2$. We have instead

$$\lambda_1 = -\frac{k_1}{c} \quad , \quad \lambda_2 = -\frac{c}{\epsilon} \quad , \quad \lambda_1 - \lambda_2 = -\frac{c}{\epsilon}.$$

and for the exponents

$$e^{-a\,\lambda_1} = 1 - \frac{a\,k_1}{c} \quad , \quad e^{a\,\lambda_2} = e^{-\frac{a\,c}{\epsilon}} = 0.$$

Using equation (16), our computations will then be

$$
\begin{aligned}
c &= \frac{k_2 c_0}{k_1\left(\frac{c}{\epsilon}\right)}\Big[\frac{k_1}{c}(1-0) - \frac{c}{\epsilon}\Big(1 - \frac{a\,k_1}{c}\Big)\Big] \\
&= \frac{k_2 c_0}{k_1\left(\frac{c}{\epsilon}\right)}\Big[- \frac{c}{\epsilon}\Big(1 - \frac{a\,k_1}{c}\Big)\Big] \\
&= \frac{k_2 c_0}{k_1 c}(ak_1 - c).
\end{aligned}
$$

We have a quadratic equation in c. i.e.

$$
\begin{aligned}
c^2 k_1 &= k_2 c_0 (ak_1 - c) \\
\Rightarrow c^2 k_1 + k_2 c_0 c - k_1 k_2 c_0 a &= 0. \qquad (27)
\end{aligned}
$$

Substituting values, we obtain the solutions for c^*,

$$c^* = 19.9,$$

which is approximately what we obtain using equation (26).

However, this value is not depicted in Figure 19, which has $c^* \approx 0.4$.

When $D = 0$, we have

$$
c\frac{dU}{dx} - k_1 U + k_2 = 0. \qquad (28)
$$

We can solve this equation to find U, followed by ΔU and finally finding c^*.

Dividing equation (28) by c:

$$
\frac{dU}{dx} - \frac{k_1}{c}U = -\frac{k_2}{c}.
$$

The integrating factor (IF) is then:

$$
\text{IF} = e^{-\int \frac{k_1}{c}\,dx} = e^{-\frac{k_1}{c}\,x}.
$$

$$
\begin{aligned}
\Rightarrow U &= e^{\frac{k_1}{c}\,x} \int -\frac{k_2}{c}\, e^{-\frac{k_1}{c}\,dx} \\
&= -\frac{k_2}{c}\, e^{\frac{k_1}{c}\,x}\big(- \frac{c}{k_1}\, e^{-\frac{k_1}{c}\,x} + \text{const}\big)
\end{aligned}
$$

$U(0) = 0 \Rightarrow$

$$\text{const} = \frac{c}{k_1}.$$

Therefore, we have

$$\begin{aligned} U &= -\frac{k_2}{c}\, e^{\frac{k_1}{c}\, x}\, \big(-\frac{c}{k_1}\, e^{-\frac{k_1}{c}\, x} + \frac{c}{k_1}\big) \\ &= \frac{k_2}{k_1}\, \big(1 - e^{\frac{k_1}{c}\, x}\big). \end{aligned} \tag{29}$$

We also have $U(\frac{a}{2}) = 0$. Hence

$$\begin{aligned} \Delta U &= U\big(\frac{a}{2}\big) - U\big(-\frac{a}{2}\big) \\ &= -\frac{k_2}{k_1}\, \big(1 - e^{\frac{a\, k_1}{2\, c}}\big). \end{aligned}$$

Using

$$c = c_0 \cdot \Delta U,$$

we then obtain

$$c = -\frac{k_2\, c_0}{k_1}\, \big(1 - e^{\frac{a\, k_1}{2\, c}}\big).$$

Assuming $\frac{a\, k_1}{2\, c} \ll 1$ and using the Taylor's expansion

$$e^{-\frac{a\, k_1}{2\, c}} = 1 - \frac{a\, k_1}{2\, c},$$

we have

$$\begin{aligned} c &= -\frac{k_2\, c_0}{k_1}\, \big(\frac{a\, k_1}{2\, c}\big) \\ \Rightarrow c^2 &= -\frac{k_2\, c_0\, a}{2} \end{aligned}$$

and finally, substituting values, we have,

$$c^* = \pm 0.27,$$

which is roughly the value shown in Figure 19. So what is the implication of this result?

Here, we have used the value of $a = 10$, which is not sufficiently big. Hence, if we plot the U profile, we will see, as shown in Figure 17, the maximum is simply less than 0.04 and not the maximum possible, which is 2. Thus, the choice of a is indeed important. If a is not sufficiently large, our U profile will not saturate to the ratio of $\frac{k_2}{k_1}$.

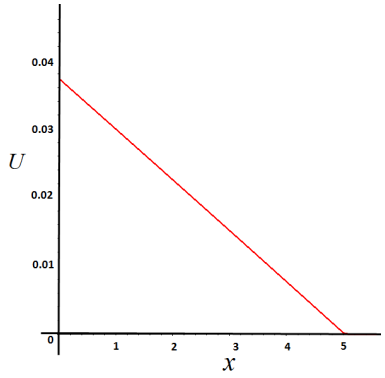

Figure 17: Concentration profile for $D = 0$.

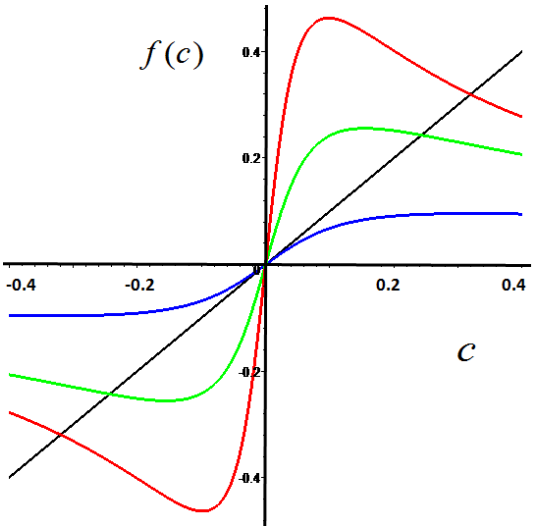

Figure 18: Plot of $f(c)$ vs c for different D using Maple. Red: $D = 1$, Green: $D = 2$, Blue: $D = 6$. Travelling solutions exist for small D but not otherwise.

On the other hand, if $D \neq 0$ and varying its value, similar as for the other parameters, will either yield a travelling solutions or otherwise. From Figure 18, we can clearly see that travelling solutions exist when D is small but not when big.

The workings to find D^*, i.e. the value of D when $c = 0$ (or the bifurcation point) will be similar to finding k_1^*. Using the first line of equation (22) and rearranging it to solve for D, we obtain

$$\begin{aligned} 4\,D^2\sqrt{\frac{k_1}{D}} &= -k_2\,c_0\,a^2 \\ 16\,D^4\,\frac{k_1}{D} &= k_2^2\,c_0^2\,a^4 \\ D^3 &= \frac{k_2^2\,c_0^2\,a^4}{16\,k_1} \\ \Rightarrow D* &= \left(\frac{k_2^2\,c_0^2\,a^4}{16\,k_1}\right)^{\frac{1}{3}}. \end{aligned} \tag{30}$$

Substituting values, we obtain the solution for D^*, i.e.

$$D^* = 5.5. \tag{31}$$

(This value is supported by Figure 19).

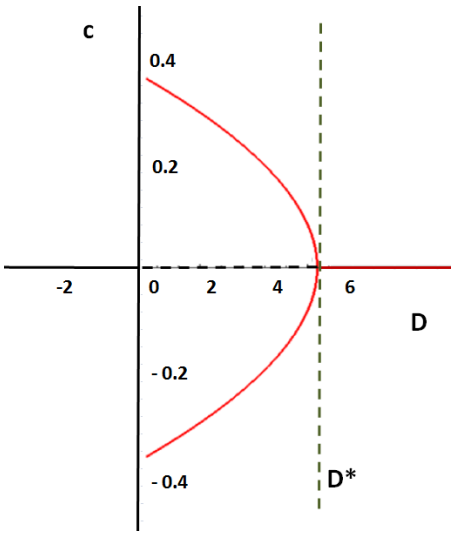

Figure 19: Plot of c vs D using Maple. The plot indicates that $c \to 0.4$ as $D \to 0$. Further, the bifurcation value of D is $D^* = 5.5$, which corresponds to the analytical estimate in equation (31).

3.5 Stability analysis of the solutions

For our model (4) and (15), we can analyse if the travelling wave solutions are stable analytically. A system is stable, if, after a tiny change or perturbation to the system, it returns to its original position after relaxation. Else, if it moves away from the original position, it is unstable. Analysing the stability of the solutions allow us to determine if the group maintain consistent uniform motion or will $c \to 0$. To derive these stability conditions, we make use of Taylor's series approximation.

We will express the time derivative of $c = f(c)$ as

$$\frac{dc}{dt} = g(c), \tag{32}$$

where $g(c) = f'(c)$.

By solving $g(c) = 0$, we are able to solve equation (32). Since we assume that $\frac{dc}{dt}$ is defined by the difference $c - f(c)$, we can let $g(c) = G\big(c - f(c)\big)$.

Therefore

$$g(c) = G\big(c - f(c)\big) = 0.$$

We then take 1^{st} order approximation. i.e.

$$G\big(c - f(c)\big) \approxeq G\big(0\big) + G'\big(0\big)\big(c - f(c)\big).$$

If $c = f(c)$, then travelling wave solutions exist. This then implies $\frac{dc}{dt} = 0$. Hence $G\big(0\big) = 0$. We can then write equation (32) as

$$\begin{aligned} \frac{dc}{dt} &= G'\big(0\big)\big(c - f(c)\big) \\ &= -\alpha\big(c - f(c)\big), \end{aligned} \tag{33}$$

where - $\alpha = G'\big(0\big)$.

Furthermore, it is reasonable to assume that $c \to f(c)$. Stability of the intersection points of $c = f(c)$ or of the travelling solutions is given by the condition that $c \to f(c) \Rightarrow \dot{c} \to 0$. We shall now analyse α and the behaviour of $c - f(c)$. We can have 2 cases. i.e.

$$c < f(c) \Rightarrow \frac{dc}{dt} > 0 \Rightarrow \alpha > 0 \tag{34}$$

or

$$c > f(c) \Rightarrow \frac{dc}{dt} < 0 \Rightarrow \alpha > 0. \tag{35}$$

By taking a linear stability analysis of a known equilibrium point, say c^*, we can further interpret the above results. If c^* is a root, then $c^* = f(c^*)$. We shall substitute $c = c^* + \epsilon$ into equation (33), where $|\epsilon| \ll 1$ is a small perturbation from c^*. i.e.

$$\begin{aligned} \frac{d(c^* + \epsilon)}{dt} &= -\alpha\big(c^* + \epsilon - f(c^* + \epsilon)\big) \\ \Rightarrow \frac{d\epsilon}{dt} &= -\alpha\big(c^* + \epsilon - f(c^* + \epsilon)\big). \end{aligned}$$

Taking 1^{st} order approximation of $f(c^* + \epsilon)$, we have

$$f(c^* + \epsilon) \approx -\alpha\big(c^* + \epsilon - f(c^*) - \epsilon f'(c^*) - O(\epsilon^2)\big).$$

The non-linear term is negligible. Thus, using $c^* = f(c^*)$, we then have

$$\frac{d\epsilon}{dt} = -\alpha\epsilon\big(1 - f'(c^*)\big).$$

We can solve for ϵ by the method of separation of variables. i.e.

$$\begin{aligned} \int \frac{d\epsilon}{dt} &= \int -\alpha\epsilon\big(1 - f'(c^*)\big)\ dt \\ \int \frac{d\epsilon}{\epsilon} &= -\alpha \int \big(1 - f'(c^*)\big)\ dt \\ ln\epsilon &= -\alpha\Big(\big(1 - f'(c^*)\big)t + const\Big) \\ \Rightarrow \epsilon(t) &= Ae^{-\alpha\Big(\big(1 - f'(c^*)\big)t\Big)}. \end{aligned}$$

For $t = 0$, $\epsilon(0) = A$. Hence

$$\epsilon(t) \quad = \quad \epsilon(0)e^{-\alpha\Big(\big(1-f'(c^*)\big)t\Big)}. \tag{36}$$

The perturbation $\epsilon(t)$ will grow unbounded for an unstable c^* or will tend to zero for a stable c^*. The sign of $f'(c^*)$ determines which is the case. For $\alpha > 0$ as shown previously, the conditions are:

$$f'(c^*) > 1 \Rightarrow \epsilon(t) \to \pm\infty \tag{37}$$

for **unstable equilibria** and

$$f'(c^*) < 1 \Rightarrow \epsilon(t) \to 0 \tag{38}$$

for **stable equilibria**.

4 Statement of the problem in 2-D medium

In the previous sections, we looked at a 1-D model. i.e. we consider a group of cells moving along a line segment of width a. Now, we shall look briefly at the case where a 2D model is used. Instead of a line segment, we consider a circle of radius $R\,(\equiv \frac{a}{2})$. We will find the solutions for U. Further analysis will not be discussed here and can be one of the areas to look into outside of this dissertation. We will consider the simplest case, i.e. of a circular group of cells moving chemotactically and assume that the circle moves along the horizontal x-axis. Our equation will be:

$$D\Big(\frac{\partial^2 U}{\partial x^2}+\frac{\partial^2 U}{\partial y^2}\Big)+c\frac{\partial U}{\partial x}-k_1U+P(x,y) \;=\; 0, \tag{39}$$

where

$$P(x,y)=\begin{cases} k_2, & x^2+y^2<R^2,\\ 0, & \text{otherwise.}\end{cases}$$

In polar coordinates we will have

$$\frac{\partial^2 U}{\partial x^2}+\frac{\partial^2 U}{\partial y^2} \;=\; \frac{\partial^2 U}{\partial r^2}+\frac{1}{r}\frac{\partial U}{\partial r}+\frac{1}{r^2}\frac{\partial^2 U}{\partial \theta^2};$$

and

$$\frac{\partial U}{\partial x} \;=\; cos\theta\frac{\partial U}{\partial r}-\frac{sin\theta}{r}\frac{\partial U}{\partial \theta}.$$

Substituting into equation (39), we have

$$D\Big(\frac{\partial^2 U}{\partial r^2}+\frac{1}{r}\frac{\partial U}{\partial r}+\frac{1}{r^2}\frac{\partial^2 U}{\partial \theta^2}\Big)+c\Big(cos\theta\frac{\partial U}{\partial r}-\frac{sin\theta}{r}\frac{\partial U}{\partial \theta}\Big)-k_1U+P(r) \;=\; 0.$$

Equation (39) is easily solved for $c=0$. In this case, due to symmetry, $U(r,\theta)=U(r)$. i.e. it does not depends on the angle. The equation in polar coordinates will now be

$$D\Big(\frac{\partial^2 U}{\partial r^2}+\frac{1}{r}\frac{\partial U}{\partial r}\Big)-k_1U+P(r) \;=\; 0, \tag{40}$$

where

$$P(r) = \begin{cases} k_2, & r < R, \\ 0, & r > R. \end{cases}$$

For the case $c \neq 0$, the computations are very tedious and cumbersome. We may need a programming software to obtain the results. Now, for the case $c = 0$, to obtained the solutions of U, we will use the **Modified Bessel function** [14]. A modified Bessel equation is of the form

$$x^2 \frac{d^2y}{dx^2} + x \frac{dy}{dx} - (x^2 + \alpha^2)\, y \;\; = \;\; 0$$

and I_0 and K_0 are the two linearly independent solutions. The solution is of the form

$$y \;\; = \;\; A\, I_0(x) + B\, K_0(x).$$

We also have $I_0 \to 0$ when $x \to 0$ and $K_0 \to \infty$ when $x = 0$.

We shall apply this Bessel function to our problem. Letting $y = U$, $x = \lambda\, r$ and dividing equation (40) by D, we obtain

$$\frac{\partial^2 U}{\partial r^2} + \frac{1}{r} \frac{\partial U}{\partial r} - \frac{k_1}{D} U \;\; = \;\; -\frac{P(r)}{D}. \tag{41}$$

The solutions will be in the form

$$U(r) = \begin{cases} U_{c_1} + U_{p_1}, & r < R, \\ U_{c_2} + U_{p_2}, & r > R, \end{cases}$$

where

$$U_c \;\; = \;\; A\, I_0(\lambda\, r) + B\, K_0(\lambda\, r).$$

and

$$U_p = \begin{cases} \frac{k_2}{k_1}, & r < R, \\ 0, & r > R. \end{cases}$$

In other words, our general solutions are

$$U(r) = \begin{cases} A_1\, I_0(\lambda\, r) + B_1\, K_0(\lambda\, r) + \frac{k_2}{k_1}, & r < R, \\ A_2\, I_0(\lambda\, r) + B_2\, K_0(\lambda\, r), & r > R. \end{cases}$$

Since $K_0(\lambda r) = 0$ for $r < R$ and $I_0(\lambda r) = 0$ for $r > R$, these simplify our general solutions to

$$U(r) = \begin{cases} A\, I_0(\lambda r) + \frac{k_2}{k_1}, & r < R, \\ B\, K_0(\lambda r), & r > R. \end{cases}$$

We will then impose boundary conditions to solve for the coefficients, A and B. i.e.

$$U_1(R) = U_2(R) \qquad \text{and} \qquad U_1'(R) = U_2'(R),$$

which then give us

$$A\, I_0(\lambda R) + \frac{k_2}{k_1} = B\, K_0(\lambda R) \tag{42}$$

and

$$A\, I_0'(\lambda R) = B\, K_0'(\lambda R). \tag{43}$$

We have a continuous 1^{st} derivative.

Since

$$\begin{aligned} I_0' &= \lambda\, I_1(\lambda r), \\ K_0' &= -\lambda\, K_1(\lambda r), \end{aligned}$$

equation (43) will then be

$$\begin{aligned} \lambda\, A\, I_1(\lambda R) &= -\lambda\, B\, K_1(\lambda R). \\ \Rightarrow A &= -B \cdot \frac{K_1(\lambda R)}{I_1(\lambda R)}. \end{aligned} \tag{44}$$

Substituting into equation (42) , we have

$$\begin{aligned} -\frac{BK_1I_0}{I_1} + \frac{k_2}{k_1} &= BK_0 \\ B\Big(K_0 + \frac{K_1I_0}{I_1}\Big) &= \frac{k_2}{k_1} \\ B &= \frac{k_2I_1}{k_1(K_0I_1 + K_1I_0)} \end{aligned} \tag{45}$$

and now substituting into equation (44), we get

$$\begin{aligned} A &= \frac{k_2 I_1 K_1}{k_1 I_1 (K_0 I_1 + K_1 I_0)} \\ &= \frac{k_2 K_1}{k_1 (K_0 I_1 + K_1 I_0)}. \end{aligned} \tag{46}$$

Thus, these give us the solution for U:

$$U(r) = \begin{cases} \frac{k_2 K_1(\lambda R)}{k_1 [K_0(\lambda R) I_1(\lambda R) + K_1(\lambda R) I_0(\lambda R)]} I_0(\lambda r) + \frac{k_2}{k_1}, & r < R, \\ \\ \frac{k_2 I_1(\lambda R)}{k_1 [K_0(\lambda R) I_1(\lambda R) + K_1(\lambda R) I_0(\lambda R)]} K_0(\lambda r), & r > R. \end{cases} \tag{47}$$

As mentioned above, we considered a circle for the model. If we are to use other fixed shapes such as a square, we will require other functions (not modified Bessel function) to solve for U.

5 Discussion

In this dissertation, a model describing a group of biological cells, which move in response to the concentration of a locally (internally) produced chemotactic agent was derived. We assumed that the cells were homotypic (cells of the same type), which is termed as a homogeneous group. The implication of the group being homogeneous, is that we assumed all cells in the group will respond equivalently to the chemotactic agent and therefore the force and resulting velocity, c, will be uniform over the group i.e. the group will move consistently given an applied force.

In order to describe the chemotactic agent, a reaction-diffusion system of linear partial differential equation to model the reacting extracellular diffusing transcript, denoted by U was used. Solving the equation gave the solutions for U for the regions, $|x| < \frac{a}{2}$ and $|x| > \frac{a}{2}$. We then plotted the U profiles for the cases $c = 0$, which gives a symmetric distribution and $c \neq 0$, which gives an asymmetric distribution; the group move left-wise for $c < 0$ (i.e. chemoattractant) and move right-wise for $c > 0$ (i.e. chemorepulsion).

We then looked at how the maximum concentration of U moves for different c and concluded that $x_{\max}$ decreases when c increases and vice versa. Next, we defined and derived the corresponding chemotaxis function, which is taken as the difference in concentration between its left and right boundaries. We denoted it as ΔU. Defining the chemotaxis function leads us to a non-linear dynamical system prescribed by an implicit function. Further, we saw that there are two possible ways to derive the function; one considering the size of the DOT, a, in the denominator of the function and, one which does not. With our expression for ΔU, we have $\Delta U \to 0$ as $c \to 0$ and $c \to \infty$. Likewise, the maximum concentration of U, i.e. $U_{\max} \to 0$ as $c \to \infty$.

After obtaining the chemotaxis function, we then analyse the effect of varying the model parameters, namely, k_1, k_2, a, c_0 and D and investigated how they effect the velocity. We examined their implications both analytically and numerically. We started off by defining c_0 as the strength of the chemotaxis. For our function to work, we need a strong c_0 and saw that $c_0 < 0$ corresponds to chemo-repulsion and $c_0 > 0$ corresponds to chemo-attraction. This is expected since our function is odd, thus we will have two solutions which are equal in magnitude but opposite in sign (corresponding to the attraction and repulsion of cells to the chemical respectively).

We also derived conditions on c_0 and the other model parameters for travelling solutions to exist. i.e. when $f'(c) > 1$ where $f(c) = c_0 \cdot \Delta U$. Our solutions are fundamentally described by the Pitchfork bifurcation, whereby, we have, at $c = 0$, a single stable stationary solution which then, at a critical value of the parameters c_0, k_1, a and D, bifurcates into two travelling solutions equal in magnitude but opposite in sign.

In almost all our computations, we used Taylor's expansion for our approximation and made certain assumptions necessary to arrive at our results. The values that we used in all our computations and substitutions are $k_1 = 0.00075, k_2 = 0.0015, a = 10, c_0 = -10$ and $D = 0.5$. For the analysis of the rate of decay, k_1, we need a small value of k_1 for a travelling solution to exist. Further, the velocity, c, saturates to a value close to 0.4 for $k_1 \to 0$. We then saw that the numerical and analytical result in finding k_1^*, i.e. the bifurcation point, differs. We obtained a numerical answer of 0.04 as opposed to the analytical result of 1.125 and 0.01 which leads us to a contradiction based on the assumptions made to obtain the result. This then supports our reliance on numerical instead of analytical result to conclude our analysis of k_1^*.

On the other hand, we need a sufficiently large a for a travelling solution to exist. In analysing a, we considered both equations (16) and (17) and arrived at different conclusions. With a in the denominator, solutions ceased to exist for values of a that is roughly less than 2.6 and greater than 517. If we use the equation without a in the denominator instead, our result shows that c saturates to a value closed to 20 as $a \to \infty$.

Taking a in the denominator into consideration has a negative implication. If we are to consider the case where the cells reacting to the chemicals are outside the DOT, we will arrive at a contradiction. For the case $x < -\frac{a}{2}$, we will have

$$\begin{aligned} c &= \frac{U(-\infty) - U(-\frac{a}{2})}{\infty} \\ &= 0. \end{aligned}$$

This result implies that there is no motion. Likewise for the case $x > \frac{a}{2}$. However if we are to use the *Cellular Potts model* instead, we will have a motion, thus a contradiction.

The last model parameter we looked at was D. For the case $D = 0$, we analysed $D \to 0$ and saw that the choice of a we used in our substitution does very much effect the results obtain analytically and numerically. If a is not sufficiently large, we saw that the maximum value of U is around 0.04, in contrast to the expected value of 2, which is the ratio of $\frac{k_2}{k_1}$. Since the value of a we used is consistent throughout, which is 10, and considered not large, we obtained the result of 0.04. Hence, the size of the DOT, a, plays a crucial role in obtaining the results.

For the case $D \neq 0$, a large D will not yield a travelling solution. Although biologist are not interested in analysing D, the diffusion coefficient, we did see that varying this parameter indeed has an effect on the chemotaxis function or the velocity, c.

All these computations, observations, analysis and conclusions are based on the fact that the chemotactic agent is internally produced i.e. we looked at a homogeneous group of cells that is attracted or repelled by a diffusing chemotactic agent it produces. If we are to consider an externally produced chemotactic agent, i.e. produced by the surrounding population of cells, rather than the group itself, we will see that the analysis that follows will be the same and mirror that for an internally produced chemical. The analysis and results are obtained by Harrison NC et.al, 2012 [4].

The equation for the reaction-diffusion system is the same as in equation (4). i.e.

$$D\frac{d^2U}{dx^2} + c\frac{dU}{dx} - k_1U + k_2 \quad = \quad 0.$$

Since the production term in the diffusion equation, k_2, is now expressed outside the group, i.e. $|x| < \frac{a}{2}$ and 0 within, i.e. $|x| > \frac{a}{2}$, the general solutions now look like

$$U = \begin{cases} Ae^{\lambda_1 x} + Be^{\lambda_2 x} + \frac{k_2}{k_1} & \text{if} \quad x < -\frac{a}{2}, \\ Ce^{\lambda_1 x} + De^{\lambda_2 x} & \text{if} \quad -\frac{a}{2} < x < \frac{a}{2}, \\ Ee^{\lambda_1 x} + Fe^{\lambda_2 x} + \frac{k_2}{k_1} & \text{if} \quad x > \frac{a}{2}, \end{cases} \tag{48}$$

and applying the same boundary and continuity conditions, we have the solutions of equation (48), i.e. for a homogeneous group with an externally produced chemotactic agent to be:

$$U = \begin{cases} \frac{k_2}{k_1(\lambda_1-\lambda_2)}\left[\lambda_2\left(e^{(x-\frac{a}{2})\lambda_1} - e^{(x+\frac{a}{2})\lambda_1}\right) + \lambda_1 - \lambda_2\right] & \text{if} \quad x \leq -\frac{a}{2}, \\ \frac{k_2}{k_1(\lambda_1-\lambda_2)}\left[\lambda_1 e^{(x+\frac{a}{2})\lambda_2} - \lambda_2 e^{(x-\frac{a}{2})\lambda_1}\right] & \text{if} \quad |x| \leq \frac{a}{2}, \\ \frac{k_2}{k_1(\lambda_1-\lambda_2)}\left[\lambda_1\left(e^{(x-\frac{a}{2})\lambda_2} - e^{(x+\frac{a}{2})\lambda_2}\right) + \lambda_1 - \lambda_2\right] & \text{if} \quad x \geq \frac{a}{2}. \end{cases}$$

Similarly, this system displays a symmetric distribution with respect to the group in a stationary frame, with its maximum concentration located centrally within the group. Further, for a travelling frame, the maximum concentration lags behind this central position proportional to the velocity of the frame, c. The expression for the location of the maximum concentration of U is identical as before, i.e.

$$x_{\max} = -\frac{ac}{2\sqrt{c^2+4k_1D}}.$$

For the chemotaxis function, c, employing the same derivation as before, we then have,

$$\begin{aligned} c &= c_0\big[U_3(\frac{a}{2}) - U_1(-\frac{a}{2})\big] \\ &= \frac{k_2c_0}{k_1(\lambda_1-\lambda_2)}\Big[\lambda_1(1-e^{a\lambda_2}) + \lambda_2(1-e^{-a\lambda_1})\Big], \end{aligned}$$

which is identical to (16).

Therefore, we can conclude that while the production dynamics of the chemotactic agent has changed from internal to external, the dynamical behaviour of the group of cells in terms of travelling solutions are equivalent.

For further discussion, there are other areas in which this dissertation can be extended. The few possible areas to look into are:

(a) considering a model for an inhomogeneous migrating group. i.e. a group that is composed of two types of cells, one that is attracted or repelled by the gradient of a locally produced, diffusing chemotactic agent, and another type within the same group that is not,

(b) considering a 2-variables model, whereby we take into account another variable, say, V, where V describes the intracellular concentration of the non-diffusible transcript called the A-mRNA. The equation for V acts as an activator to model the concentration of A-mRNA. We will have

$$V = \begin{cases} 1, & \text{inside DOT} \\ 0, & \text{outside DOT} \end{cases},$$

and the equation is given by

$$\frac{dV}{dx} = cV' - k_3V,$$

where k_3 is the rate of A-mRNA decay,

(c) the proof underlying the existence of one maximum for the chemotaxis function instead of multiple maximums,

(d) extending the analysis using 2-D model (as being discussed in the 1-D model).

Hence, there are indeed room to widen the scope of this dissertation in the future.

References

[1] Harrison NC, Diez del Corral R, Vasiev B (2011) Coordination of Cell Differentiation and Migration in Mathematical Models of Caudal Embryonic Axis Extension. PLoS ONE 6(7):e22700. doi:10.1371/journal.pone.0022700

[2] Neilson M, Mackenzie J.A, Webb S.D, Insall R.H Modelling cell movement and chemotaxis using pseudopod-based feedback.

[3] Alexander P (1999-2004), Stan M (2004) Non-linear Dynamical system. Theoretical Biology & Bioinformatics, Utrecht University, Utrecht.

[4] Harrison NC (2012) Chapter 2: 1D Continuous models of a migrating group.

[5] Vasieva O, Rasolanjanahary M, Vasiev B (2012) Mathematical modelling in developmental biology.

[6] Harrison NC (2008) Modelling the Regression of Henson's Node using a modified Cellular Potts model.

[7] Keller E.F, Segel L.A (1971) Model for Chemotaxis. J Theor. Biol. 30, 225 234.

[8] Vasiev B.N, Hogeweg P, Panfilov A.V (1994) Simulation of Dictyostelium Discoideum Aggregation via Reaction-Diffusion Model. Physical Review Letters Vol 73, No. 23.

[9] I.D. Goldberg Cell motility factors, Birkhäuser (1991), "2 – 3".

[10] B.Dennis Cell Movements, Garland Publishing, INC. New York & London (1992), "295, 304".

[11] Green's Function. Retrieved 2nd July 2012. From http://en.wikipedia.org/wiki/Green 27s function

[12] Pitchfork Bifurcation. Retrieved 2nd July 2012. From http://en.wikipedia.org/wiki/Pitchfork bifurcation

[13] Chemotaxis. Retrieved 28th August 2012. From http://en.wikipedia.org/wiki/Chemotaxis

[14] Bessel function. Retrieved 10th September 2012. From http://en.wikipedia.org/wiki/Bessel function

A Maple codes

A.1 Plotting the concentration profile

```
lambda[1] := (-c+sqrt(c^2+4*k[1]*d))/(2*d);
lambda[2] := (-c-sqrt(c^2+4*k[1]*d))/(2*d);

U1 :=k[2]*lambda[2]*((exp(lambda[1]*(x-(a/2)))-
 exp(lambda[1]*(x+(a/2)))))/(k[1]*(lambda[1]-lambda[2]));

U2:=(k[2]*(lambda[2]*exp(lambda[1]*(x-(a/2)))-
lambda[1]*exp(lambda[2]*(x+(a/2)))+(lambda[1]-
lambda[2])))/(k[1]*(lambda[1]-lambda[2]));

U3 :=k[2]*lambda[1]*((exp(lambda[2]*(x-(a/2)))-
exp(lambda[2]*(x+(a/2)))))/(k[1]*(lambda[1]-lambda[2]));
```

A.1.1 For $c = 0$ (stationary profile)

```
k[1] := 0.75e-3; k[2] := 2*k[1]; c := 0; d := .5; a := 50;
with(plots, implicitplot);
plot([piecewise(x <= -a/2, U1,
And(-a/2 <= x, x <= a/2), U2, x >= a/2, U3)],
x = -100 .. 100, y=0..1.3, labels=[x,U]);
```

A.1.2 For $c > 0$ (repulsion)

```
k[1] := 0.75e-3; k[2] := 2*k[1]; c := 0.015; d := .5; a := 50;
with(plots, implicitplot);
plot([piecewise(x <= -a/2, U1,
And(-a/2 <= x, x <= a/2), U2, x >= a/2, U3)],
x = -100 .. 100, y=0..1.3, labels=[x,U]);
```

A.1.3 For $c < 0$ (attraction)

```
k[1] := 0.75e-3; k[2] := 2*k[1]; c := -0.015; d := .5; a := 50;
with(plots, implicitplot);
plot([piecewise(x <= -a/2, U1,
And(-a/2 <= x, x <= a/2), U2, x >= a/2, U3)],
x = -100 .. 100, y=0..1.3, labels=[x,U]);
```

A.1.4 For $D = 0$

```
k[1] := 0.75e-3; k[2] := 2*k[1]; c := 0.2; d := .0001; a := 10;
with(plots, implicitplot);
plot([piecewise(x <= -a/2, U1,
And(-a/2 <= x, x <= a/2), U2, x >= a/2, U3)],
x = 0 .. 6, y=0..0.05, labels=[x,U]);
```

A.2 Plotting the location of maximum concentration of U

```
x[max]:= -(c*a)/(2*sqrt(c^2+4*k[1]*d));

G:= subs(a=50, k[1]=0.75e-3, d=.5,x[max]);

plot(G,c=-0.2..0.2);
```

A.3 Plotting the chemotaxis function ($f(c)$ vs c)

```
y2:=(k[2]*c0*(lambda[1]*(1-exp(a*lambda[2]))+
lambda[2]*(1-exp(-a*lambda[1]))))/(k[1]*(lambda[1]-lambda[2]));
```

A.3.1 Varying c_0

```
with(plots):

f0(c):=c;
d1(c):=subs(k[1]= 0.75e-3, k[2]= 1.5e-3,d = .5,a= 10, c0=-10., y2):
d2(c):=subs(k[1]= 0.75e-3, k[2]= 1.5e-3,d = .5,a= 10, c0=-7., y2):
d3(c):=subs(k[1]= 0.75e-3, k[2]= 1.5e-3,d = .5,a= 10, c0=-3., y2):
plots[multiple](plot, [d1(c), c = -.1 .. .1, color=red, linestyle =1],
[d2(c), c=-.1.. .1, color=green, linestyle=1],
[d3(c), c = -.1 .. .1, color=blue, linestyle=1],
[f0(c),c=-.1.. .1,color=black], labels =[c,f(c)]);
```

A.3.2 Varying k_1

```
with(plots):

f0(c):=c;
g1(c):=subs(k[1]= 45e-3, k[2]= 1.5e-3,d = .5,a= 10, c0=-10,y2):
g2(c):=subs(k[1]= 20e-3, k[2]= 1.5e-3,d = .5,a= 10,c0=-10, y2):
```

```
g3(c):=subs(k[1]= 10e-3, k[2]= 1.5e-3,d = .5,a= 10,c0=-10, y2):
plots[multiple](plot, [g1(c), c = -.4 .. .4, color=red],[g2(c),
c=-.4.. .4, color=green],[g3(c), c = -.4 .. .4, color=blue],
f0(c),c=-.4.. .4,color=black], labels =[c,f(c)]);
```

A.3.3 Varying a

```
with(plots):

f0(c):=c;
f1(c):=subs(k[1]= 0.75e-3, k[2]= 1.5e-3,d = .5,a= 10, c0=-10., y2):
f2(c):=subs(k[1]= 0.75e-3, k[2]= 1.5e-3,d = .5,a= 5, c0=-10., y2):
f3(c):=subs(k[1]= 0.75e-3, k[2]= 1.5e-3,d = .5,a= 2.5, c0=-10., y2):
plots[multiple](plot, [f1(c), c = -.1 .. .1, color=red, linestyle =1],
[f2(c), c=-.1.. .1, color=green, linestyle=1],
[f3(c), c = -.1 .. .1, color=blue, linestyle=1],
[f0(c),c=-.1.. .1,color=black], labels =[c,f(c)]);
```

A.3.4 Varying D

```
with(plots):

f0(c):=c;
m1(c):=subs(k[1]= 0.75e-3, k[2]= 1.5e-3,d = 1,a= 10,c0=-10, y2):
m2(c):=subs(k[1]= 0.75e-3, k[2]= 1.5e-3,d = 2,a= 10, c0=-10,y2):
m3(c):=subs(k[1]= 0.75e-3, k[2]= 1.5e-3,d = 6,a= 10, c0=-10,y2):
plots[multiple](plot, [m1(c), c = -.4 .. .4, color=red],
[m2(c), c=-.4.. .4, color=green],
[m3(c), c = -.4 .. .4, color=blue],
[f0(c),c=-.4.. .4,color=black], labels =[c,f(c)]);
```

A.4 Plotting the velocity (c) against the model parameters

A.4.1 c vs c_0

```
y2:=(k[2]*c0*(lambda[1]*(1-exp(a*lambda[2]))+
lambda[2]*(1-exp(-a*lambda[1]))))/(k[1]*(lambda[1]-lambda[2]));

BifPlot:=(eval(c*(c0/y2),[k[1]=0.00025,k[2]=0.0005,d=0.5,a=50]));
plot(BifPlot,c=-0.05..0.05,c0=-5..5);
```

A.4.2 c vs k_1

```
with(plots);
with(ExcelTools);
with*ArrayTools

V := [[0, 0]];
for A from 0.1e-2 by 0.1e-2 to 0.5e-1 do
sol := fsolve(c = eval(c0*k[2]*(lambda[1]*(1-exp(a*lambda[2]))
+lambda[2]*(1-exp(-a*lambda[1])))/(k[1]*(lambda[1]-lambda[2])),
[k[1] = A, k[2] = 0.15e-2, a = 10, c0 = -10, d = .5]), {c = 0 .. 5});

V := [op(V), [A, rhs(op(1, sol))]]
end do

pointplot(V);
V[2]

FileTools[Remove]("c_vs_k[1].xls");
Export(convert(V, Array), "c_vs_k[1].xls", "v", "B1")
```

A.4.3 c vs a

(i) With 'a' in the denominator:

```
with(plots);
with(ExcelTools);
with*ArrayTools

V := [[0, 0]];
for A from 3 by 10 to 600 do
sol := fsolve(c = eval(c0*k[2]*(lambda[1]*(1-exp(a*lambda[2]))
+lambda[2]*(1-exp(-a*lambda[1])))/(a*k[1]*(lambda[1]-lambda[2])),
[k[1] = 0.75e-3, k[2] = 0.15e-2, d = .5, c0 = -10, a = A]), {c = 0 .. .4});

V := [op(V), [A, rhs(op(1, sol))]]
end do

pointplot(V);
V[60];

FileTools[Remove]("c_vs_a_with_a_new.xls");
Export(convert(V, Array), "c_vs_a_with_a_new.xls", "v", "B1")
```

(ii) Without 'a' in the denominator:

```
with(plots);
with(ExcelTools);
with*ArrayTools

V := [];
for A by 10000 to 1000000 do
sol := fsolve(c = eval(c0*k[2]*(lambda[1]*(1-exp(a*lambda[2]))
+lambda[2]*(1-exp(-a*lambda[1])))/(k[1]*(lambda[1]-lambda[2])),
[k[1] = 0.75e-3, k[2] = 0.15e-2, d = .5, c0 = -10, a = A]), {c = 0 .. 21});

V := [op(V), [A, rhs(op(1, sol))]]
end do;

pointplot(V);

FileTools[Remove]("c_vs_a_new.xls");
Export(convert(V, Array), "c_vs_a_new.xls", "v", "B1")
```

A.4.4 c vs D

```
with(plots);
with(ExcelTools);
with*ArrayTools

V := [[0, 0]];
for Dif from 0.1e-2 by .1 to 10 do
sol := fsolve(c = eval(c0*k[2]*(lambda[1]*(1-exp(a*lambda[2]))
+lambda[2]*(1-exp(-a*lambda[1])))/(k[1]*(lambda[1]-lambda[2])),
[k[1] = 0.75e-3, k[2] = 0.15e-2, a = 10, c0 = -10, d = Dif]), {c = 0 .. 1});

V := [op(V), [Dif, rhs(op(1, sol))]]
end do

pointplot(V);
V[6];

FileTools[Remove]("c_vs_d.xls");
Export(convert(V, Array), "c_vs_d.xls", "v", "B1")
```

* the data was exported to excel before plotting.